

On non-dissipative wave–mean interactions in the atmosphere or oceans

By OLIVER BÜHLER AND MICHAEL E. McINTYRE

Centre for Atmospheric Science at the Department of Applied Mathematics and Theoretical Physics, University of Cambridge, Silver Street, Cambridge CB3 9EW, UK
<http://www.atm.ch.cam.ac.uk/cas/>

(Received 22 June 1997 and in revised form 8 September 1997)

Idealized model examples of non-dissipative wave–mean interactions, using small-amplitude and slow-modulation approximations, are studied in order to re-examine the usual assumption that the only important interactions are dissipative. The results clarify and extend the body of wave–mean interaction theory on which our present understanding of, for instance, the global-scale atmospheric circulation depends (e.g. Holton *et al.* 1995). The waves considered are either gravity or inertia–gravity waves. The mean flows need not be zonally symmetric, but are approximately ‘balanced’ in a sense that non-trivially generalizes the standard concepts of geostrophic or higher-order balance at low Froude and/or Rossby number. Among the examples studied are cases in which irreversible mean-flow changes, capable of persisting after the gravity waves have propagated out of the domain of interest, take place without any need for wave dissipation. The irreversible mean-flow changes can be substantial in certain circumstances, such as Rossby-wave resonance, in which potential-vorticity contours are advected cumulatively. The examples studied in detail use shallow-water systems, but also provide a basis for generalizations to more realistic, stratified flow models. Independent checks on the analytical shallow-water results are obtained by using a different method based on particle-following averages in the sense of ‘generalized Lagrangian-mean theory’, and by verifying the theoretical predictions with nonlinear numerical simulations. The Lagrangian-mean method is seen to generalize easily to the three-dimensional stratified Boussinesq model, and to allow a partial generalization of the results to finite amplitude. This includes a finite-amplitude mean potential-vorticity theorem with a larger range of validity than had been hitherto recognized.

1. Introduction

A notoriously difficult yet fundamental problem in chemical, climate and weather prediction is how to represent the effects of small-scale atmospheric waves in numerical simulations of the global atmospheric circulation – the so-called gravity-wave parametrization problem. The importance of this problem has been recognized by the World Climate Research Programme (WCRP) through its Committee on Gravity Wave Processes and their Parametrization, under the WCRP sub-programme on Stratospheric Processes and their Role in Climate (SPARC). It is not known whether gravity waves have comparable significance for ocean circulations, but in our present state of knowledge of ocean dynamics it cannot be safely assumed that gravity waves are insignificant.

Gravity waves are too small in spatial scale to be directly represented in the simulations. Instead, their effects have to be indirectly represented using parametrization schemes based on approximate results derived from the so-called ‘wave–mean interaction theory’, which provides approximations to the effects of the waves upon the larger scales, all the way up to the global scale of the stratospheric circulation.

The wave–mean interaction theory used in gravity-wave parametrizations relies on a certain ‘dissipation assumption’, saying that all the significant wave effects can be represented as mean forces that depend on wave breaking and other forms of wave dissipation. Conversely, whenever and wherever the waves are not dissipating, it is assumed that they can be altogether ignored. In this paper we re-examine the dissipation assumption, and show by careful analysis that cases exist, in an idealized model context at least, in which the assumption is misleading.

The cases of non-dissipative interactions to be studied turn out to be conceptually interesting from a wider perspective as well. At first sight it would appear natural (e.g. McIntyre & Norton 1990) to regard the ‘mean flow’ in these problems as a ‘balanced’ flow in the usual sense to which the idea of ‘potential vorticity inversion’ applies (Hoskins, McIntyre & Robertson 1985; McIntyre 1993). However, although the concept of a balanced mean flow does indeed turn out to be applicable to the wave–mean problems studied here, it will be seen that this requires a non-trivial generalization of the usual ideas about balanced flow evolution, as will be outlined now.

We recall, to begin with, that the decomposition of a given flow into a balanced, potential-vorticity-controlled part and an unbalanced, gravity-wave-like part has long been recognized as a useful conceptual and numerical tool in atmosphere and ocean dynamics. Numerically, describing the balanced part of the flow accurately and efficiently may well require a different numerical technique to that used to describe the (unbalanced) gravity waves. For instance, current global atmospheric simulations handle gravity waves in a manner completely different from their main flow evolution scheme, namely via the parametrization schemes already mentioned.

Conceptually, the decomposition allows the very special characteristics of potential vorticity (PV) and its evolution to be exploited. The relevant definitions of the two-dimensional shallow-water PV and of the Rossby–Ertel PV for three-dimensional stratified flow are, respectively,

$$q \equiv \frac{\nabla \times \mathbf{u} + f}{h} \quad \text{and} \quad Q \equiv \frac{(\nabla \times \mathbf{u} + f\hat{z}) \cdot \nabla \theta}{\rho}, \quad (1.1)$$

where \mathbf{u} is the velocity field, f is the Coriolis parameter, h is the height of the shallow-water layer, \hat{z} is the vertical unit vector, θ is potential temperature, and ρ is density. In the absence of forcing and dissipation PV is materially conserved, i.e.

$$\frac{Dq}{Dt} = 0 \quad \text{and} \quad \frac{DQ}{Dt} = 0, \quad (1.2)$$

which makes obvious the necessity of forcing or dissipation to change the value of PV on material particles. The (unbalanced) gravity waves, on the other hand, have no essential dependence on PV. It can be noted in passing that the distinction between the balanced part and the gravity waves is clear-cut only in the linear limit of small disturbances to a steady state, the so called ‘Rossby adjustment problem’. If the disturbances are not small then finding the best possible such distinction at low

† In the left-hand equation $\nabla \times \mathbf{u}$ is shorthand for $\hat{z} \cdot (\nabla \times \mathbf{u})$, and use is made repeatedly of the fact that in two dimensions $\nabla \times \mathbf{u}$ can be treated as a (pseudo-)scalar.

Froude and/or Rossby number is still very much a matter of current research, and indeed subject, probably, to ultimate limitations (e.g. Norton 1988).

The picture we generally have to deal with is one in which the flow evolution is a side-by-side evolution of the balanced part together with the gravity waves, and in which each side is coupled to the other through a two-way interaction. The coupling may be weak in many situations of practical interest, but, as noted above, is known to be essential for the long-term evolution of the atmosphere. The first half of the coupling, the effect of the balanced part of the flow on the evolution of the gravity waves, can to first approximation be studied using linear wave theory. It can lead to, for instance, the generation, refraction, reflection, and dissipation of gravity waves. In the limit of a slowly varying mean flow most of these effects can be modelled using standard ray-tracing techniques, which hence form the basis of current parametrization schemes. The other half of the coupling, the effect of the gravity waves on the evolution of the balanced part of the flow, is arguably less well understood, and still requires some careful consideration.

If gravity waves were altogether absent – let us call this a notional ‘perfectly balanced model’ – the flow evolution can be thought of in two distinct steps (cf. Hoskins *et al.* 1985). Given the PV at a given time, the *diagnostic* step allows calculation of the balanced flow fields, including the balanced velocity fields, from the PV. Thereafter, the *prognostic* step advances the PV field, usually by simply advecting it with the balanced velocity field. This leads to a changed PV field and the cycle starts again. Because in a perfectly balanced model the flow is entirely controlled by the PV, the diagnostic step is often called PV inversion.

How can the presence of gravity waves change this picture of the evolution of the balanced part? The gravity waves will, in principle, affect both steps in the balanced evolution sketched above, as we shall show. This is outside the scope of the traditional dissipation assumption, which implies, not always correctly, that the waves affect only the prognostic step, and then only when the waves are dissipating or breaking. The new results of this paper suggest that the non-dissipative effect of the gravity waves on the balanced part of the flow should be taken into account by a suitable modification of the diagnostic step, because, in some cases at least, this effect is substantial.

In other words, simple PV inversion has to be non-trivially generalized to a diagnostic procedure that recognizes the joint importance not only of PV but also of certain averaged properties of the gravity waves, to yield the balanced part of the velocity field that is used in the prognostic advection step of the PV. In such a procedure, the simple condition of balance between, say, the Coriolis force and the pressure gradient is generalized to take gravity-wave effects into account that, on average, modify this balance condition.

Most of the small-amplitude results of this paper are contained in two equations expressing modified diagnostic steps for the simplest possible balance condition, namely quasi-geostrophic balance, in the two-dimensional shallow-water system and in the three-dimensional Boussinesq system. These equations are, respectively, of the form

$$\left(\nabla^2 - \frac{1}{L_R^2}\right) \Psi^L = \bar{q}^L - q_0 + \nabla \times \mathbf{p}_2 - \frac{A}{c_0 L_R} E \quad (1.3)$$

and

$$\Psi_{xx}^L + \Psi_{yy}^L + \frac{f_0^2}{N^2} \Psi_{zz}^L = \left(\bar{Q}^L - Q_0\right) N^{-2} + [\nabla \times \mathbf{p}_2] \cdot \hat{\mathbf{z}} \quad (1.4)$$

In both equations Ψ^L is a stream function for the horizontal Lagrangian-mean velocity

field, and the evolution of the Lagrangian-mean PVs \bar{q}^L and \bar{Q}^L is entirely determined by the advection with the velocities corresponding to Ψ^L . The background PV fields are denoted by q_0 and Q_0 , L_R is the shallow-water Rossby deformation length, c_0 is the speed of high-frequency shallow-water gravity waves, A is a factor dependent on the intrinsic gravity-wave frequency (cf. (6.6)), N is the buoyancy frequency in the Boussinesq system, E is the average shallow-water wave energy density, and \mathbf{p}_2 is the gravity-wave pseudomomentum vector in both cases. Both E and \mathbf{p}_2 are $O(a^2)$ ‘wave properties’, i.e. they can be evaluated from a knowledge of zeroth-order mean flow and linear, $O(a)$ gravity-wave fields alone, where $a \ll 1$ is the relevant small wave amplitude.

These equations differ from the standard quasi-geostrophic equations by the additional terms containing E and \mathbf{p}_2 , which describe the wave-induced changes in the Lagrangian-mean velocity field. In general, these changed Lagrangian-mean velocities will lead to deformations of contours of \bar{q}^L (or \bar{Q}^L) that would not have taken place without the gravity waves. Because these deformations persist once the gravity waves have propagated out of the domain of interest, it is possible to speak of *irreversible* changes in the PV, and thereby in the mean flow, that are induced by non-dissipating gravity waves. Only in the special case of constant PV, in which material advection cannot change the PV field, would the wave-induced changes in the mean flow be reversible.

It can be shown that, in principle, there is no *a priori* bound on the size of PV changes that can be achieved in this way, even in the limit of small-amplitude gravity waves. This is demonstrated below through an example of Rossby-wave resonance, in which the wave-induced PV changes produce a positive feedback that re-enforces the cumulative deformation of PV contours. It is this point, namely that $O(a^2)$ changes in the mean velocities induced by non-dissipative gravity waves may result in cumulative, dynamically significant displacements of PV contours (growing as $O(a^2 t)$ in the resonant example), that is missed when the dissipation assumption is simply taken for granted.

The plan of the paper is as follows. In §2 the set-up of a shallow-water beta-channel is described that provides the simplest possible model in which non-dissipative wave–mean interaction effects can be studied. In §3 a perturbation expansion for small-amplitude gravity waves in this beta-channel is presented, which leads to explicit equations describing the entire $O(a^2)$ mean-flow response as well as to equations describing only the balanced part of the $O(a^2)$ mean flow. The definition of ‘mean flow’ used there is a slow-modulation average over the rapidly varying phase of the gravity waves, which includes Rossby waves as mean flows. Note that using a ‘mean’ and ‘disturbance’ formalism simplifies the mathematical equations, but that it does not provide a clear-cut physical distinction between balanced and unbalanced parts of the flow. For instance, there may well be large-scale, mean gravity waves.

The balanced part of the mean-flow evolution driven by the gravity waves is investigated in detail in §4, including the resonant case. The problem is then reconsidered by using the particle-following formalism of generalized Lagrangian-mean theory (GLM) in §5. GLM theory is fully defined and described in Andrews & McIntyre (1978*a, b*), hereafter referred to as AM78*a, b*), but a self-contained outline of the features of the theory used here is also presented in §5. A major clarification of the origin of the result (1.3) is achieved in this way, providing not only an independent check on its validity, but also pointing to generalizations to other flow systems such as the Boussinesq, stratified model. Furthermore, (1.3) can be seen as a small-amplitude consequence of a fully nonlinear PV theorem in GLM theory. Interestingly, the practical usefulness

of this nonlinear PV theorem seems to extend to forced and dissipative flows as well, a fact that has not been recognized before.

In §6 certain extensions and modifications of the simplest shallow-water model are explored in order to probe the robustness of the interaction effects, and in §7 the threads are drawn together to suggest a simple model of balanced evolution in which dissipative and non-dissipative gravity-wave effects are both recognized. Nonlinear numerical simulations in §8 provide a further independent check on the results. It turns out, however, that the standard shallow-water model is not useful for the highly non-dissipative simulations needed, owing to dissipative effects connected with the rapid formation of gravity wave shocks in this model. Therefore, a modification of the kind presented in §6 is chosen for the simulations, which prevents gravity-wave shock formation in a simple, non-dissipative manner (Bühler 1997), and permits accurate non-dissipative numerical experiments.

Section 9 derives the result (1.4) for a three-dimensional stratified fluid system. This is a vital step towards understanding the corresponding effects in the context of stratified fluid systems, which are of direct relevance to actual atmosphere or ocean dynamics. The section provides first a Boussinesq version of the nonlinear PV theorem, and then derives the small-amplitude result (1.4). Concluding remarks are given in §10. An Appendix supplements §§3 and 6 with details of the evolution of the mean height field in the shallow-water system, including a detailed discussion of the importance of correct $O(a^2)$ boundary conditions, which prove vital, for instance, in certain one-dimensional wave–mean interaction problems.

2. Set-up of the shallow-water beta-channel

The two-dimensional shallow-water system is the simplest flow model in which both gravity waves and vortical features occur, and in which concepts such as balance and wave–mean interactions involving gravity waves are non-trivial. Using a flat, tangent-plane shallow-water system avoids non-essential complications due to the curvature of the Earth. Such a shallow-water system can easily be equipped with a background PV gradient in the meridional (i.e. northward–southward) direction either through a latitude-dependent Coriolis parameter (the so-called beta-effect), or through latitude-dependent shear of a suitable background flow in the zonal (i.e. eastward–westward) direction. This leads to well-defined background PV contours with undisturbed alignment parallel to the zonal direction.

Such a beta-channel set-up is depicted in figure 1. It can be thought of as an idealized mid-latitude ‘stratosphere’. Simple boundary conditions are provided by periodicity in the x (zonal) direction and impermeable walls in the y (meridional) direction. The period length in the x -direction is L and is assumed to be comparable to the channel width D . The impermeable channel walls are not fixed but oscillate in a prescribed manner (not depicted) to generate coherent wavetrains of small-scale gravity waves with wavenumber magnitude κ . These wavetrains form a sequence of parallel rays that stretch obliquely across the channel. The envelope scale of the rays is comparable to the period length L , and it is assumed that the ray envelope is slowly varying on the scale of the waves, i.e. $1/(\kappa L) \ll 1$ is the relevant small ‘JWKB’ or slow-modulation parameter. An alternating pattern of northward- and southward-pointing rays is chosen in anticipation of interesting effects occurring when the pattern projects strongly onto the Rossby-wave modes of the channel. In addition to the meridional gradient of the Coriolis parameter $f = f_0 + \beta y$, a steady background zonal flow $U(y)$ in geostrophic balance may be present. Its meridional

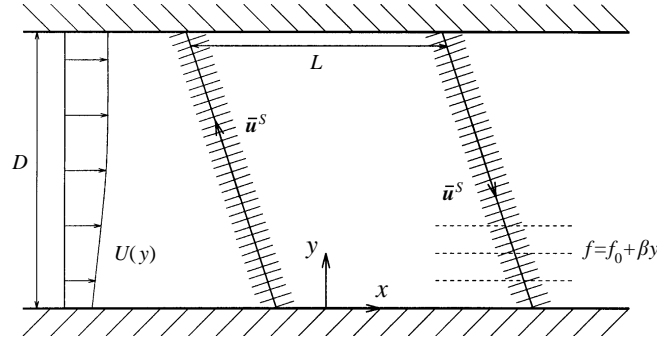


FIGURE 1. The shallow-water beta-channel set-up. D is the width of the channel, L is the period length in the zonal direction, (x, y) are cartesian coordinates in the zonal (along the channel) and meridional (across the channel) directions, $U(y)$ is the background zonal flow, f is the varying Coriolis parameter, and \bar{u}^S is the Stokes drift of the gravity waves. The short lines perpendicular to the Stokes drift vector indicate individual phase lines of the gravity waves.

Physical meaning	Small quantity	Small parameter
Small-amplitude gravity waves	$h'_1, \kappa u'_1 /\hat{\omega}$	a
Large† Rossby deformation length $L_R \equiv c_0/f_0$	L/L_R	ϵ
Slowly varying channel and ray envelope	$1/(\kappa L)$	μ
Weak background PV-gradient	$\beta D/f_0$	$\mu \min\{1, \epsilon^{-2}\}$
Background flow in quasi-geostrophic balance	$\mathcal{U}/(f_0 D)$	$\mu \min\{1, \epsilon^{-2}\}$

† This assumption will be relaxed in §6.

TABLE 1. Scalings and small parameters for the channel set-up

profile is either constant or slowly varying on the scale of the gravity waves. The scaling of the various parameters is summarized in table 1.

The gravity waves are assumed to be of sufficiently small amplitude to allow a useful perturbation expansion of all flow fields in powers of the small wave amplitude $a \ll 1$. The JWKB parameter $1/(\kappa L) \ll 1$, which expresses a scale separation between the rapidly varying phase of the gravity waves and the envelope scale of the wavetrain, is assumed to be small enough to allow a unique decomposition of all flow fields into slowly varying mean parts and rapidly varying disturbance parts. Therefore, the mean part of a given flow field is defined as the Eulerian average over the rapidly varying phase of the gravity waves. Clearly, using a scale separation to define the mean flow is exact only in the limit of infinite scale separation. This is unlike, for instance, a mean-flow definition based on zonal averaging, which is always exact. Therefore, in practice it has to be assumed, in the usual way, that the scale separation is sufficiently large for the definition of the mean fields to work with negligible error.

With these assumptions the flow fields can be uniquely decomposed into their mean and disturbance parts at the relevant orders in small wave amplitude a . This decomposition is denoted by $\phi = \bar{\phi} + \phi'$ and $\bar{\phi}' \equiv 0$, where the overbar denotes the Eulerian mean and ϕ stands for any flow field. Contributions at first and second order in wave amplitude a are denoted by a corresponding subscript, whereas $O(1)$ contributions are denoted by capital letters. For example

$$\mathbf{u}' = \mathbf{u}'_1 + O(a^2) \quad \text{and} \quad \bar{\mathbf{u}} = \mathbf{U} + \bar{\mathbf{u}}_2 + O(a^3), \quad (2.1)$$

where \mathbf{u} is the velocity vector.

The two-dimensional momentum equation for shallow-water flow without dissipation or forcing is

$$\frac{D\mathbf{u}}{Dt} + f\hat{\mathbf{z}} \times \mathbf{u} + c_0^2 \nabla h = 0 \quad \text{with} \quad f = f_0 + \beta y, \quad (2.2)$$

where the Coriolis parameter f includes the beta-effect. Here D/Dt is the material derivative, $\mathbf{u} = (u, v)$ is the velocity field, $\hat{\mathbf{z}}$ is the unit vector normal to the (x, y) -plane, c_0 is the speed of high-frequency gravity waves,† and h is the non-dimensional depth of the layer such that $h = 1$ corresponds to the undisturbed layer depth.

Taking the divergence and the curl of the momentum equation gives the standard divergence and vorticity equations, which together with the mass-continuity equation form the set that will be considered in most of this paper, i.e.

$$\frac{Dh}{Dt} + h\nabla \cdot \mathbf{u} = 0, \quad (2.3)$$

$$\frac{\partial \nabla \cdot \mathbf{u}}{\partial t} + \nabla \cdot [(\mathbf{u} \cdot \nabla)\mathbf{u}] - f\nabla \times \mathbf{u} + \beta u + c_0^2 \nabla^2 h = 0, \quad (2.4)$$

$$\frac{D\nabla \times \mathbf{u}}{Dt} + \beta v + (f + \nabla \times \mathbf{u})\nabla \cdot \mathbf{u} = 0. \quad (2.5)$$

It turns out that it is computationally simpler to work with (2.5) instead of the PV equation (1.1).

The above equations will be used to determine the flow fields at three orders of magnitude in wave amplitude a , namely $O(a^0)$, $O(a^1)$, $O(a^2)$, which will provide an ordering of the flow into background, waves, and mean-flow response. Specifically, this will lead to an $O(1)$ steady zonal background flow in geostrophic balance, to $O(a)$ gravity waves, and to an $O(a^2)$ mean-flow response to the gravity waves. As further small parameters appear (see table 1) one could attempt higher-order expansions in those other small parameters as well. However, this is not done in the present paper, and only the relevant leading-order contributions with respect to all other small parameters will be retained. The small parameters of the problem are summarized in table 1. There h'_1 is the non-dimensional gravity-wave depth disturbance, \mathbf{u}'_1 is the gravity-wave velocity disturbance, $\kappa = (k^2 + l^2)^{1/2}$ is the magnitude of the wavenumber vector $\mathbf{k} = (k, l)$ of the small-scale gravity waves, $\hat{\omega}$ is their intrinsic frequency, β is the meridional gradient of f , and \mathcal{U} is the velocity scale of the background flow. Note that because $D \sim L$ has been assumed, the roles of D and L for the scaling are interchangeable. The small quantities above scale with their associated small parameters, e.g. $h'_1 \sim a$.

It turns out to be highly convenient, in the first instance, to restrict the parameter ϵ , which measures the size of the channel against the so-called Rossby deformation length L_R , to values of much less than unity. This implies that large-scale mean flows behave as if there were an almost rigid upper lid on the channel, which allows the convenient neglect of all mean-flow depth changes. It also implies, together with the JWKB assumption $\mu = 1/(\kappa L) \ll 1$, that only high-frequency gravity waves (i.e. waves with $\hat{\omega} \gg f_0$), need to be considered, which will simplify certain relations regarding the wave structure. However, neither of these two points is essential for the working of the theory and in §6 the restriction $\epsilon \ll 1$ will be relaxed, which will be seen to lead to important and qualitatively new wave–mean interaction features. This is already

† The wave speed c_0 is related to the gravity acceleration g and the undisturbed shallow-water layer depth H by $c_0^2 = gH$, but it turns out that g and H are never needed separately and hence only c_0 is introduced.

accounted for in table 1, as it will turn out (cf. (3.1) below) that a tighter bound on U and β is useful in the cases where ϵ is not small.

Using the small JWKB parameter μ for several other small quantities is of some computational convenience, because it avoids unnecessarily cumbersome notation when no detailed exploration of complicated parameter regimes is intended. The background flow may vary slowly in the meridional y -direction, but then its derivative scales with the channel width, i.e.

$$U_y \sim \mathcal{U}/D \quad \text{and} \quad U_{yy} \sim \mathcal{U}/D^2, \text{ etc.} \quad (2.6)$$

This scaling allows the background-flow vorticity gradient U_{yy} to be of the same order as β . Note therefore that although $U_y \ll f$ nevertheless $U_{yy} \sim f_y$, which is important to keep in mind when collecting all relevant leading-order terms in the equations below.

3. Expansion in small wave amplitude

3.1. Background flow

A non-zero $U(y)$ will, in the presence of background rotation, require a varying depth field $h = 1 + \Delta H(y)$ to compensate for the Coriolis force. However, the necessary depth-field variation $\Delta H(y)$ will be minutely small for a weak background flow $U(y)$ that obeys the scaling in table 1, and will be neglected. This can be demonstrated by inserting $U(y)$ into the steady y -momentum equation,

$$c_0^2 \frac{d\Delta H}{dy} = -(f_0 + \beta y)U(y) \quad \Rightarrow \quad \Delta H \sim \frac{f_0 D \mathcal{U}}{c_0^2} \sim \mu \min\{\epsilon^2, 1\}. \quad (3.1)$$

3.2. Gravity waves

The $O(a)$ continuity, divergence, and vorticity equations are

$$D_t h'_1 + \nabla \cdot \mathbf{u}'_1 = 0, \quad (3.2)$$

$$D_t \nabla \cdot \mathbf{u}'_1 + c_0^2 \nabla^2 h'_1 - f \nabla \times \mathbf{u}'_1 = -2U_y \frac{\partial v'_1}{\partial x} - \beta u'_1, \quad (3.3)$$

$$D_t \nabla \times \mathbf{u}'_1 + (f - U_y) \nabla \cdot \mathbf{u}'_1 = -v'_1 (\beta - U_{yy}), \quad (3.4)$$

where D_t is the $O(1)$ material derivative

$$D_t \equiv \frac{\partial}{\partial t} + U(y) \frac{\partial}{\partial x}. \quad (3.5)$$

The continuity and vorticity equations can be integrated if linearized particle displacements are introduced. These are defined (e.g. AM78a or Andrews, Holton & Leovy 1987) by

$$D_t(\xi', \eta') \equiv (u'_1, v'_1) + (\xi' \cdot \nabla)U = (u'_1 + \eta' U_y, v'_1). \quad (3.6)$$

The scale of these displacements is $|\xi'| \sim a/\kappa$. From (3.6) it follows that

$$\nabla \cdot \mathbf{u}'_1 = D_t \nabla \cdot \xi' - (\xi' \cdot \nabla)(\nabla \cdot U) = D_t \nabla \cdot \xi'. \quad (3.7)$$

Together with the fact that $D_t U = D_t f \equiv 0$, equations (3.6) and (3.7) allow integration of (3.2) and (3.4) along $O(1)$ material trajectories. If we assume that there was no disturbance at the initial time, then the constants of integration can be set to zero. This yields

$$h'_1 + \nabla \cdot \xi' = 0 \quad (3.8)$$

and

$$\nabla \times \mathbf{u}'_1 - (f - U_y)h'_1 = -\eta'(\beta - U_{yy}). \quad (3.9)$$

This integral of the $O(a)$ vorticity equation makes the stretching and advecting of background vorticity obvious. For the scaling in table 1 the stretching term is much bigger than the advection term. Together, (3.2) and (3.9) imply that the size of $\nabla \times \mathbf{u}'_1$ relative to $\nabla \cdot \mathbf{u}'_1$ is $f_0/\hat{\omega}$.

The scaling $\epsilon \ll 1$ in table 1 implies that the wavelength of the gravity waves is small compared to L_R and that therefore the intrinsic gravity-wave frequency satisfies $\hat{\omega}^2 \gg f_0^2$. However, this scaling requirement for ϵ will be relaxed in §6 below, and it proves convenient to derive the gravity-wave structure here for all frequencies, including frequencies near f_0 . Such low-frequency waves feel both gravitational and Coriolis forces and are called inertia-gravity waves.

It is assumed that β and all derivatives of U are negligible for the local structure of the small-scale, near-plane gravity waves, which, for instance, implies $D_t \xi' = \mathbf{u}'_1$ in (3.6). Substituting (3.2) and (3.9) in (3.3) gives the familiar inertia-gravity-wave dispersion relation

$$\hat{\omega}^2 = f_0^2 + c_0^2 \kappa^2. \quad (3.10)$$

The intrinsic gravity-wave phase velocity $c \equiv \hat{\omega}/\kappa$ and the intrinsic group velocity $c_g \equiv ((\partial \hat{\omega}/\partial k)^2 + (\partial \hat{\omega}/\partial l)^2)^{1/2}$ magnitudes are

$$\frac{c^2}{c_0^2} = \left(1 - \frac{f_0^2}{\hat{\omega}^2}\right)^{-1} \quad \text{and} \quad \frac{c_g^2}{c_0^2} = \left(1 - \frac{f_0^2}{\hat{\omega}^2}\right)^{+1}, \quad (3.11)$$

respectively. Both intrinsic phase and group velocities are parallel to the local wavenumber vector \mathbf{k} . The wave structure depends only on \mathbf{k} , and assuming without loss of generality that $\mathbf{k} = (k, 0)$ it is straightforward to show that u'_1 and h'_1 oscillate in phase with each other and out of phase with v'_1 . Furthermore

$$\mathbf{k} = (k, 0) \quad \Rightarrow \quad \nabla \times \mathbf{u}'_1 = v'_{1,x}, \quad h'_1 + \xi'_{,x} = 0, \quad v'_1 + f_0 \xi' = 0 \quad (3.12)$$

follow from (3.8) and (3.9). The quadratic correlations

$$\mathbf{k} = (k, 0) \quad \Rightarrow \quad \overline{u_1'^2} = \overline{v_1'^2} + c_0^2 \overline{h_1'^2} \quad \text{and} \quad \overline{v_1'^2} = \frac{f_0^2}{\hat{\omega}^2} \overline{u_1'^2} \quad (3.13)$$

hold, together with $\hat{\omega}^2 \overline{\xi'^2} = \overline{u_1'^2}$ and $\hat{\omega}^2 \overline{\eta'^2} = \overline{v_1'^2}$. The non-dimensional wave amplitude $a \ll 1$ measures the relative size of the nonlinear terms in the equations with respect to the linear terms. A suitable definition of a is $a \sim |\mathbf{u}'_1|/c$, or, equivalently in this model, $a \sim h'_1$, as in table 1.

The standard intrinsic wave-energy density per unit mass E , its partition into kinetic and potential wave energy, and its evolution equation can be derived most directly from the linearized momentum and continuity equations. This gives

$$E \equiv \frac{1}{2} \left(\overline{|\mathbf{u}'_1|^2} + c_0^2 \overline{h_1'^2} \right) = O(a^2 c^2), \quad (3.14)$$

$$\overline{|\mathbf{u}'_1|^2} = \left(1 + \frac{f_0^2}{\hat{\omega}^2}\right) E, \quad c_0^2 \overline{h_1'^2} = \left(1 - \frac{f_0^2}{\hat{\omega}^2}\right) E, \quad (3.15)$$

$$D_t E + \overline{u'_1 v'_1} U_y = -c_0^2 \nabla \cdot \overline{(h'_1 \mathbf{u}'_1)} \equiv -c_0^2 \nabla \cdot \overline{\mathbf{u}'_2}. \quad (3.16)$$

There is no contribution from the Coriolis terms in (3.16), as these cannot do any

work on the fluid. The loss of equipartition of wave energy in (3.15) is typical for the influence of the Coriolis force, i.e. it also occurs for inertia-gravity waves in other flow models such as the three-dimensional Boussinesq model. It can be seen that low-frequency waves have less average potential energy (i.e. less $c_0^2 \overline{h_1'^2}$) than average kinetic energy. The limiting case $f_0^2/\hat{\omega}^2 \rightarrow 1$ is that of inertial oscillations, in which all wave energy is kinetic.

Because h_1' is in phase only with the velocity component parallel to \mathbf{k} , the Stokes drift vector $\bar{\mathbf{u}}_2^S \equiv \overline{(h_1' \mathbf{u}_1')}$ can be simply related to E by

$$\bar{\mathbf{u}}_2^S = \frac{\mathbf{k}}{\hat{\omega}} E, \quad (3.17)$$

which implies that $\bar{\mathbf{u}}_2^S = O(a^2 c)$. This definition of $\bar{\mathbf{u}}_2^S$ is consistent with the standard definition of Stokes drift as the difference between Lagrangian-mean and Eulerian-mean velocity, as will be shown in §5. The immediate significance of $\bar{\mathbf{u}}_2^S$ here is brought out by considering the normalized total mean mass flux at a fixed point

$$\overline{h\mathbf{u}} = \overline{h\bar{\mathbf{u}}} + \overline{h'\mathbf{u}'} = \bar{h}_2 \mathbf{U} + \bar{\mathbf{u}}_2 + \bar{\mathbf{u}}_2^S + O(a^3). \quad (3.18)$$

This equation will be important later when the $O(a^2)$ boundary conditions at the channel walls are considered. Note that large values of $\nabla \cdot \bar{\mathbf{u}}_2^S$ are linked with gravity-wave transience via (3.16).

The ‘JWKB’ approximation based on $\kappa L \gg 1$ allows the use of standard ray-tracing methods (e.g. Whitham 1974; Andrews *et al.* 1987) to calculate $\mathbf{k}(x, y, t)$ and the amplitude of the gravity-wave field that develops from the wall undulations. In that approximation (3.16) can be rewritten as

$$\left(\frac{\partial}{\partial t} + \left[U \hat{\mathbf{x}} + c_g \frac{\mathbf{k}}{\kappa} \right] \cdot \nabla \right) \left(\frac{E}{\hat{\omega}} \right) + \left(\frac{E}{\hat{\omega}} \right) \nabla \cdot \left[U \hat{\mathbf{x}} + c_g \frac{\mathbf{k}}{\kappa} \right] = 0, \quad (3.19)$$

which expresses the conservation of so-called ‘wave action’, whose density per unit mass is $E/\hat{\omega}$. The quantity in square brackets is the absolute group velocity, which includes the background velocity. Rays are integral curves of this velocity field. The background quantities $f(y)$ and $U(y)$ are independent of x and t , and therefore $k = \mathbf{k} \cdot \hat{\mathbf{x}}$ and $\hat{\omega} + Uk$ are constant along rays. Changes of $\hat{\omega}$ and $l = \mathbf{k} \cdot \hat{\mathbf{y}}$ along rays are therefore linked to changes in Uk , and for the scaling in table 1 these changes are negligible. This implies that rays are straight lines and that if rays start parallel at the site of wave generation, then they remain parallel as they cross the channel. This means that the divergence $\nabla \cdot [\dots] = 0$ in (3.19), i.e.

$$\left(\frac{\partial}{\partial t} + \left[U \hat{\mathbf{x}} + c_g \frac{\mathbf{k}}{\kappa} \right] \cdot \nabla \right) E = 0, \quad (3.20)$$

holds approximately with the group velocity $[\dots]$ constant along rays. Therefore E is simply advected with constant group velocity along straight parallel rays.

If $\epsilon \ll 1$ then $f_0^2 \ll \hat{\omega}^2$, and hence $c \approx c_g \approx c_0$. Therefore, under this scaling the gravity waves are nearly irrotational, non-dispersive waves.

3.3. Mean-flow response

The mean $O(a^2)$ vorticity equation is (cf. (2.5))

$$D_t \nabla \times \bar{\mathbf{u}}_2 + \bar{v}_2 (\beta - U_{yy}) + (f - U_y) \nabla \cdot \bar{\mathbf{u}}_2 = -\nabla \cdot (\overline{\mathbf{u}_1' \nabla \times \mathbf{u}_1'}). \quad (3.21)$$

The forcing term can be related to $\bar{\mathbf{u}}_2^S$ by using the leading-order expression for $\nabla \times \mathbf{u}'_1$ from (3.9) to obtain

$$\nabla \times \mathbf{u}'_1 = (f - U_y) h'_1 \quad (3.22)$$

$$\Rightarrow \overline{\mathbf{u}'_1 \nabla \times \mathbf{u}'_1} = (f - U_y) \bar{\mathbf{u}}_2^S \quad (3.23)$$

$$\Rightarrow -\nabla \cdot \overline{(\mathbf{u}'_1 \nabla \times \mathbf{u}'_1)} = -\bar{v}_2^S (\beta - U_{yy}) - (f - U_y) \nabla \cdot \bar{\mathbf{u}}_2^S. \quad (3.24)$$

It can be checked that retaining the smaller advection term from (3.9) would only add a much smaller term than either of the two terms on the right-hand side of (3.24).

Now, consider the leading-order generalized Lagrangian-mean velocity (AM78a), which is defined as

$$\bar{\mathbf{u}}_2^L \equiv \bar{\mathbf{u}}_2 + \bar{\mathbf{u}}_2^S. \quad (3.25)$$

It is clear that, because $\bar{\mathbf{u}}_2^S$ is already determined by the $O(a)$ gravity-wave field, knowledge of $\bar{\mathbf{u}}_2^L$ implies knowledge of $\bar{\mathbf{u}}_2$ and vice versa. Unlike $\bar{\mathbf{u}}_2$, which is the Eulerian-mean velocity at a fixed position, $\bar{\mathbf{u}}_2^L$ is the Lagrangian-mean velocity following a fixed particle. One can express (3.21) in terms either of $\bar{\mathbf{u}}_2^L$ or of $\bar{\mathbf{u}}_2$. These equations are, respectively,

$$\left. \begin{aligned} D_t \nabla \times \bar{\mathbf{u}}_2 + \bar{v}_2 (\beta - U_{yy}) + (f - U_y) \nabla \cdot \bar{\mathbf{u}}_2 &= -\bar{v}_2^S (\beta - U_{yy}) - (f - U_y) \nabla \cdot \bar{\mathbf{u}}_2^S, \\ D_t \nabla \times \bar{\mathbf{u}}_2^L + \bar{v}_2^L (\beta - U_{yy}) + (f - U_y) \nabla \cdot \bar{\mathbf{u}}_2^L &= D_t \nabla \times \bar{\mathbf{u}}_2^S. \end{aligned} \right\} \quad (3.26)$$

This makes conspicuous the fact that equation (3.21) is more easily expressed in terms of $\bar{\mathbf{u}}_2^L$ than in terms of $\bar{\mathbf{u}}_2$. It is intriguing to note the difference in the appearance of the forcing terms in the two equations. Disregarding divergence parts for the moment, the *Eulerian*-mean flow appears to be forced through advection of background vorticity by the Stokes drift (the first term on the right-hand side). On the other hand, the *Lagrangian*-mean flow appears to be forced by the transience of the curl of the Stokes drift, which does not involve the background vorticity at all. Of course, $\bar{\mathbf{u}}_2$ and $\bar{\mathbf{u}}_2^L$ satisfy different boundary conditions, a fact that is clearly important in judging which quantity is more convenient to use as a dependent variable. The boundary conditions along the channel axis are periodicity in all fields, which applies to $\bar{\mathbf{u}}_2^L$ as well as to $\bar{\mathbf{u}}_2$. However, at the channel walls the mass flux across the walls must be zero, and it is here that the boundary conditions differ. From (3.18) one obtains

$$\overline{hw} = \bar{v}_2 + \bar{v}_2^S + O(a^3) = \bar{v}_2^L + O(a^3) = 0 \quad \text{at } y = 0 \text{ and } y = D. \quad (3.27)$$

This mean boundary condition should strictly be applied at the mean position of the wall (cf. AM78a), but to leading order the mean position of the wall coincides with the undisturbed wall position. It follows that \bar{v}_2^L is zero at the walls whereas $\bar{v}_2 = -\bar{v}_2^S$ there. This is another reason to favour the Lagrangian-mean velocity as dependent variable, because it satisfies a simple, homogeneous boundary condition, regardless of whether gravity waves are present or not.

From now on the Lagrangian-mean velocity $\bar{\mathbf{u}}_2^L$ will be made the basis of the investigation. In practice this means that $\bar{\mathbf{u}}_2^S$ is regarded as given and $\bar{\mathbf{u}}_2^L$ is sought as a response to it. This also means that the term ‘mean-flow response’ from now on refers to $\bar{\mathbf{u}}_2^L$ instead of $\bar{\mathbf{u}}_2$.

The mean $O(a^2)$ continuity equation is (cf. (2.3))

$$D_t \bar{h}_2 + \nabla \cdot \bar{\mathbf{u}}_2 = -\nabla \cdot \overline{h'_1 \mathbf{u}'_1} \quad \text{or} \quad D_t \bar{h}_2 + \nabla \cdot \bar{\mathbf{u}}_2^L = 0. \quad (3.28)$$

The absence of any apparent mass sinks or sources in the second form in (3.28) is another strong reason to favour the choice of $\bar{\mathbf{u}}_2^L$ over $\bar{\mathbf{u}}_2$ as a dependent variable.

Using (3.28) and $D_t(f - U_y) = 0$ the vorticity equation (3.26) can be rewritten as

$$D_t [\nabla \times \bar{\mathbf{u}}_2^L - (f - U_y)\bar{h}_2] + \bar{v}_2^L (\beta - U_{yy}) = D_t \nabla \times \bar{\mathbf{u}}_2^S. \quad (3.29)$$

The mean $O(a^2)$ divergence equation is (cf. (2.4))

$$D_t \nabla \cdot \bar{\mathbf{u}}_2 + c_0^2 \nabla^2 \bar{h}_2 - f \nabla \times \bar{\mathbf{u}}_2 + 2U_y(\bar{v}_2)_x + \beta \bar{u}_2 = -\nabla \cdot \left[\overline{(\mathbf{u}'_1 \cdot \nabla) \mathbf{u}'_1} \right]. \quad (3.30)$$

The wave-induced forcing term on the right can be re-written as follows:

$$\left. \begin{aligned} \overline{(\mathbf{u}'_1 \cdot \nabla) \mathbf{u}'_1} &= \nabla \frac{1}{2} \overline{\mathbf{u}'_1{}^2} + \overline{(\nabla \times \mathbf{u}'_1) \hat{\mathbf{z}} \times \mathbf{u}'_1} = \nabla E/2 + (f - U_y) \hat{\mathbf{z}} \times \bar{\mathbf{u}}_2^S \\ -\nabla \cdot \left[\overline{(\mathbf{u}'_1 \cdot \nabla) \mathbf{u}'_1} \right] &= -\nabla^2 E/2 - (\beta - U_{yy}) \bar{u}_2^S + (f - U_y) \nabla \times \bar{\mathbf{u}}_2^S, \end{aligned} \right\} \quad (3.31)$$

where (3.9) has again been used. Inserting this expression back into (3.30), adding $D_t \nabla \cdot \bar{\mathbf{u}}_2^S$ and another Stokes-drift term, and using (3.28) and (3.16) then gives

$$\begin{aligned} & - (D_t D_t - c_0^2 \nabla^2) \bar{h}_2 + 2U_y(\bar{v}_2^L)_x + \beta \bar{u}_2^L \\ &= - (D_t D_t + \frac{1}{2} \nabla^2 c_0^2) \frac{E}{c_0^2} + f \nabla \times \bar{\mathbf{u}}_2^L + 2U_y(\bar{v}_2^S)_x - U_y \nabla \times \bar{\mathbf{u}}_2^S + U_{yy} \bar{u}_2^S. \end{aligned} \quad (3.32)$$

In contrast with the vorticity and continuity equations, introducing $\bar{\mathbf{u}}_2^L$ did not lead to any simplification here. Also equation (3.32) looks complicated because it contains terms of very different magnitude. The equation can be simplified whilst retaining the relevant leading-order terms by neglecting all background terms involving U or β . This is possible because the dominant scale in (3.32) is set by the much larger terms containing c_0^2 . The simplified (3.32) is (after an overall sign change)

$$\left(\frac{\partial^2}{\partial t^2} - c_0^2 \nabla^2 \right) \bar{h}_2 + f_0 \nabla \times \bar{\mathbf{u}}_2^L = \left(\frac{\partial^2}{\partial t^2} + c_0^2 \frac{\nabla^2}{2} \right) \frac{E}{c_0^2}. \quad (3.33)$$

The boundary conditions for \bar{h}_2 at the walls arise in the usual way from the condition $\bar{v}_2^L = 0$ there, and are given in the Appendix.

In principle, the three linear equations (3.28), (3.29), and (3.33) together with appropriate boundary conditions for $\bar{\mathbf{u}}_2^L$ and \bar{h}_2 determine the entire $O(a^2)$ mean-flow response to the wave-induced forcing represented by E and $\nabla \times \bar{\mathbf{u}}_2^S$. In the usual way, these linear equations have one balanced mode and two unbalanced modes, and the balanced part of the velocity field $\bar{\mathbf{u}}_2^L$ is mainly described by $\nabla \times \bar{\mathbf{u}}_2^L$, and the unbalanced part of $\bar{\mathbf{u}}_2^L$ is mainly described by $\nabla \cdot \bar{\mathbf{u}}_2^L$.

This motivates decomposing $\bar{\mathbf{u}}_2^L$ into a rotational non-divergent part associated with $\nabla \times \bar{\mathbf{u}}_2^L$ and an irrotational divergent part associated with $\nabla \cdot \bar{\mathbf{u}}_2^L$. In the usual way, the homogeneous wall boundary conditions can be applied to each part individually without loss of generality. It remains to determine the non-divergent irrotational constant zonal flow component of $\bar{\mathbf{u}}_2^L$. In a zonally periodic, doubly connected domain this can be achieved by specifying the circulation along a particular curve that reaches from $x = 0$ to $x = L$. Consider the material line that coincides with the southern wall. It turns out (as can be easily verified using the formalism of GLM theory in §5) that the $O(a)$ undulations of this contour may lead to $O(a^2)$ changes in the mean circulation associated with $\bar{\mathbf{u}}_2^L$ along the wall boundary. These changes arise partly because of the non-zero background rotation and partly because of the Lagrangian averaging process. However, this circulation change is uniformly bounded in time, and reverses back to zero when the waves are switched off and the wall returns to its

original position. Furthermore, there is no background zonal PV gradient on which a uniform zonal flow in $\bar{\mathbf{u}}_2^L$ could act to produce a change in the PV distribution. Therefore the constant zonal flow component of $\bar{\mathbf{u}}_2^L$ will be neglected. It can be noted that simplifying $\bar{\mathbf{u}}_2^L$ based on the criterion of whether or not a component of $\bar{\mathbf{u}}_2^L$ is able to create irreversible, lasting changes in the PV distribution will be the vital ingredient for the accurate development of balanced mean-flow equations below.

Consider now a ‘spin-up’ of the gravity-wave field from an initial steady state without waves. If it is assumed in (3.29) that the size of $\nabla \times \bar{\mathbf{u}}_2^L$ is comparable to the size of $\nabla \times \bar{\mathbf{u}}_2^S = O(a^2 c_0/L)$, then (3.33) implies that \bar{h}_2 is comparable to $E/c_0^2 = O(a^2)$ at leading order. This in turn implies by (3.28) that, in terms of size, $\nabla \cdot \bar{\mathbf{u}}_2^L \sim \nabla \times \bar{\mathbf{u}}_2^L$ if the spin-up is sufficiently fast so that $D_t \sim c_0/L$. This is the timescale necessary to send a gravity wave across the channel, which appears reasonable for the spin-up, and hence it is clear that $\nabla \cdot \bar{\mathbf{u}}_2^L$ cannot be neglected against $\nabla \times \bar{\mathbf{u}}_2^L$ simply on order-of-magnitude grounds.

However, once the waves have settled to a steady state, the evolution of the mean flow can be expected to occur on a much slower timescale dictated by Rossby-wave dynamics, i.e. $D_t = O(\beta L)$ then. The slowly evolving height field is then approximately described by (3.33) without the time derivatives, i.e.

$$-\nabla^2 \bar{h}_2 + \frac{f_0}{c_0^2} \nabla \times \bar{\mathbf{u}}_2^L = \frac{\nabla^2 E}{2 c_0^2}. \quad (3.34)$$

The steady wave energy term on the right-hand side corresponds to a steady change of $O(a^2)$ in the height field \bar{h}_2 , which in this model tends to decrease the height field within the gravity wavetrain. Note that under the assumption $L \ll L_R$ (i.e. $\epsilon \ll 1$ in table 1) this change in \bar{h}_2 dominates the usual quasi-geostrophic change of $O(a^2 \epsilon)$. Under the same assumption $(f - U_y)\bar{h}_2$ can be neglected against $\nabla \times \bar{\mathbf{u}}_2^L$ in (3.29), which corroborates the scaling assumption for $\nabla \times \bar{\mathbf{u}}_2^L$ made previously.

Therefore, it can be seen that the divergent part of $\bar{\mathbf{u}}_2^L$ has led to a significant change in \bar{h}_2 , which is directly linked to the presence of the gravity waves. However, this change is approximately reversible, i.e. if the waves are imagined to spin down again then the changes in \bar{h}_2 are approximately undone. Looked at from another way, this means that the mean material displacements associated with $\nabla \cdot \bar{\mathbf{u}}_2^L$, which correspond to pushing particles together or apart to produce the changes in \bar{h}_2 , are approximately reversible. This picture only neglects free $O(a^2)$ mean gravity waves that may be excited by the transient spin-up or spin-down of the $O(a)$ gravity waves and which would continue propagating along the channel after the $O(a)$ waves had spun down again. However, these propagating $O(a^2)$ gravity waves would by their very nature also produce only reversible mean material displacements.

In summary, the entire $O(a^2)$ mean response consists of a balanced part and an unbalanced, gravity-wave-like part. The unbalanced part does create significant material displacements associated with significant depth changes \bar{h}_2 , but these material displacements depend on the continued presence of the $O(a)$ gravity waves and are therefore reversible. The balanced part, on the other hand, creates significant mean material displacements that persist after the $O(a)$ gravity waves have disappeared. These balanced mean material displacements are therefore the only displacements that can lead to irreversible, lasting changes in the PV distribution. From these considerations it can be argued, first, that only the balanced part of the $O(a^2)$ mean-flow response needs to be considered in order to calculate irreversible mean material displacements, and, second, that \bar{h}_2 and $\nabla \cdot \bar{\mathbf{u}}_2^L$ can be entirely neglected for the

evolution of this balanced part. The second part of this statement will need some modification once the restriction $L \ll L_R$ is relaxed in §6, but the first part of it will remain valid.

Hence, from now on \bar{h}_2 and $\nabla \cdot \bar{\mathbf{u}}_2^L$ will be neglected. This decouples the vorticity equation from the other two equations and results in a simple balanced system of the usual quasi-geostrophic kind, i.e.

$$\boxed{D_t(\nabla \times \bar{\mathbf{u}}_2^L) + \bar{v}_2^L (\beta - U_{yy}) = D_t(\nabla \times \bar{\mathbf{u}}_2^S) \quad \text{and} \quad \nabla \cdot \bar{\mathbf{u}}_2^L = 0} \quad (3.35)$$

together with $\bar{v}_2^L = 0$ at the walls.

The diagnostic and prognostic steps of this balanced system can be made apparent by introducing a quantity \tilde{q} defined as

$$\tilde{q} \equiv f_0 + \beta y - U_y + \nabla \times (\bar{\mathbf{u}}_2^L - \bar{\mathbf{u}}_2^S), \quad (3.36)$$

and this definition, together with $\nabla \cdot \bar{\mathbf{u}}_2^L = 0$ and the boundary conditions, forms the diagnostic step, or the balance condition, of the balanced system. Equation (3.35) now implies that to $O(a^2)$

$$\boxed{\left(\frac{\partial}{\partial t} + (U + \bar{u}_2^L) \frac{\partial}{\partial x} + \bar{v}_2^L \frac{\partial}{\partial y} \right) \tilde{q} = 0}, \quad (3.37)$$

which forms the prognostic step of the balanced system, expressing the invariance of \tilde{q} along mean material trajectories.

The quantity \tilde{q} is closely related to the usual shallow-water PV given by (1.1); in fact it can be shown using GLM theory (AM78a and §5 below) that (1.1) in general implies the invariance of \bar{q}^L , the Lagrangian-mean of q , along mean material trajectories. Therefore, to $O(a^2)$ the quantities \tilde{q} and \bar{q}^L satisfy the same differential equation. If the flow starts from an initial state without gravity waves then \tilde{q} and \bar{q}^L are equal initially and hence throughout the evolution. In this case the important result

$$\boxed{\bar{q}^L = \tilde{q} = f_0 + \beta y - U_y + \nabla \times (\bar{\mathbf{u}}_2^L - \bar{\mathbf{u}}_2^S)} \quad (3.38)$$

holds to $O(a^2)$. The occurrence of $\bar{q}^L \equiv \nabla \times (\bar{\mathbf{u}}_2^L - \bar{\mathbf{u}}_2^S)$ neatly captures the $O(a^2)$ changes in the mean PV field, a fact that is not at all obvious from the definition of q in (1.1).

The origin of (3.36), (3.37) and (3.38) will be substantially clarified in §5 below, where the exact particle-following averaging formalism of GLM theory is used.

4. Mean-flow response: irreversibility and resonance

In (3.35) the background-shear gradient $-U_{yy}$ adds naturally to the background gradient of f . Although the assumed scaling allows the two terms to be of the same order – which may itself lead to interesting effects – the simplest solutions are obtained by setting U to a constant because this results in an equation with constant coefficients. This is done from now on. First $U = 0$ is considered, and then U is set to a positive constant.

4.1. Zero background flow $U = 0$

For the scenario envisaged here, the picture that emerges from (3.35) is that of episodes of slow evolution (when the gravity-wave field, and hence $\bar{\mathbf{u}}_2^S$, is steady) that are punctuated by brief intervals of rapid transience when the gravity-wave field is

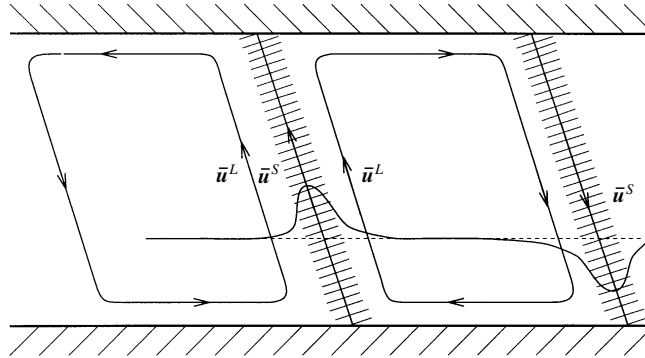


FIGURE 2. The flow situation immediately after the spin-up of the gravity waves. $\nabla \times \bar{u}_2^L = \nabla \times \bar{u}_2^S$, but \bar{u}_2^L and \bar{u}_2^S satisfy different boundary conditions at the channel walls. The broken line and the solid line indicate the initial and current position of a PV contour advected by \bar{u}_2^L .

spinning up or down. In the slow episodes the right-hand side of (3.35) is zero (as $U = 0$), and hence \bar{u}_2^L satisfies an unforced Rossby-wave operator, i.e. it evolves as a simple superposition of free Rossby-wave channel modes. During transient spin-up or spin-down (3.35) becomes approximately

$$\frac{\partial}{\partial t} \nabla \times \bar{u}_2^L = \frac{\partial}{\partial t} \nabla \times \bar{u}_2^S. \quad (4.1)$$

Figure 2 illustrates the flow pattern created by (4.1) just after spin-up of the gravity waves. The curls of \bar{u}_2^L and \bar{u}_2^S are equal but the fields satisfy different boundary conditions at the wall forcing regions. The difference between the two fields (which is the Eulerian mean velocity \bar{u}_2) is therefore irrotational, non-divergent, and forced by inhomogeneous wall boundary conditions with zonal scale L . The difference therefore has modal structure $\exp(iKx)\exp(\pm Ky)$ with $K = O(1/L)$, which implies that significant differences between \bar{u}_2^L and \bar{u}_2^S are confined to a boundary layer near the wall, and otherwise decay exponentially with envelope scale L in the meridional direction away from the wall. Far away from the wall, i.e. at distances $\geq L$, the material velocity \bar{u}_2^L is therefore approximately equal to the Stokes drift \bar{u}_2^S . This results in the characteristic circulation cells depicted in figure 2.

Also depicted is a PV contour at its initial position (broken line) and at a displaced position (solid line). PV contours are material lines and hence simply advected by the $O(a^2)$ mean material velocity \bar{u}_2^L . (The $O(a)$ rapid undulations directly due the gravity waves are not depicted.)

If $\beta = 0$, i.e. if there is no pre-existing PV gradient, then the initial state produced by (4.1) is a steady state of (3.35). This means that after the transient spin-up there is no further acceleration of the mean flow. If the gravity waves are imagined to spin down in a similar way as they spun up, then there would be no mean flow left behind. Although material particles would have changed their positions, i.e. the time integral of \bar{u}_2^L would be non-zero in most places, this would have produced no dynamically relevant change. This corroborates the expectation that no irreversible mean-flow changes are possible in the absence of a pre-existing PV gradient, as stated in the introduction.

If, on the other hand, $\beta \neq 0$, then material displacements will act on a pre-existing PV gradient and will lead to an irreversible change in the PV field. Initially, $\bar{u}_2^L \approx \bar{u}_2^S$ near the centre of the channel and hence the size of the PV anomalies thus created

grows initially as $\beta \bar{v}_2^L \approx \beta \bar{v}_2^S$. However, if $\beta \neq 0$, then $\nabla \times (\bar{\mathbf{u}}_2^L - \bar{\mathbf{u}}_2^S) = 0$ is not a steady state of (3.35), i.e. the flow continues to evolve on a slow timescale after the rapid spin-up. The solution of (3.35) for initial conditions such as those depicted in figure 2 is given by a slowly evolving dispersive Rossby wavetrain, whose spatial scale is $O(L)$ and whose timescale is therefore $O(1/(\beta L))$ or longer. The Rossby-wave dynamics will periodically reverse all velocities and material displacements. The maximal PV disturbance that is achieved depends on the initial conditions for $\nabla \times \bar{\mathbf{u}}_2^L$ and is hence bounded by the size of $\nabla \times \bar{\mathbf{u}}_2^S$. If the gravity waves are spun down again, then there will always be finite undulations of PV contours that are left behind, and consequently the flow would not revert back to its original rest state. This exhibits the essential link between a non-zero background PV gradient ($\beta - U_{yy}$) in (3.35) and irreversible, lasting mean-flow changes, i.e. changes that do not revert to zero once the waves have come and gone.

4.2. Non-zero background flow $U > 0$ and resonance

If U is equal to a non-zero constant, then the slow evolution of (3.35) is modified. In a frame moving with the background flow the gravity-wave field now translates with speed $-U$ in the zonal direction, and if $U > 0$ this translation speed may match the phase speed of a free Rossby-wave channel mode, which is always negative, and resonance may occur.

This is most easily demonstrated by introducing a stream function Ψ^L for $\bar{\mathbf{u}}_2^L$ such that $\hat{\mathbf{z}} \times \nabla \Psi^L \equiv \bar{\mathbf{u}}_2^L$ and $\nabla^2 \Psi^L = \nabla \times \bar{\mathbf{u}}_2^L$. After the spin-up the evolution of Ψ^L is described by (cf. (3.35))

$$\left(\frac{\partial}{\partial t} + U \frac{\partial}{\partial x} \right) \nabla^2 \Psi^L + \beta \frac{\partial \Psi^L}{\partial x} = U \frac{\partial}{\partial x} \nabla \times \bar{\mathbf{u}}_2^S \quad (4.2)$$

with

$$\nabla^2 \Psi^L|_{t=0} = \nabla \times \bar{\mathbf{u}}_2^S. \quad (4.3)$$

The normal modes of Ψ^L have spatial structure $\exp(iKx) \sin(yn\pi/D)$, where K is the zonal wavenumber and n is the meridional mode number. The homogeneous wall boundary conditions are satisfied if n is an integer. A resonant mode exists if there exists a meridional mode number n^* such that the spatial part of the Rossby-wave operator in (4.2) is zero, the condition for which is

$$\frac{\beta}{U} = K^2 + \left(\frac{n^* \pi}{D} \right)^2. \quad (4.4)$$

For this mode (4.2) predicts resonant growth of $\nabla^2 \Psi^L$, i.e. $\nabla^2 \Psi^L \propto t$ with growth rate proportional to the size of $\nabla \times \bar{\mathbf{u}}_2^S$. The mean PV equation (3.38) then shows that $\bar{q}_2^L \propto t$ as well. In the simplest possible case $\bar{u}_2^S = 0$ and $\bar{v}_2^S = \frac{1}{2} a^2 c_0 \sin(Kx)$, and then the time T until \bar{q}_2^L of the resonant mode has grown to the size of $\nabla \times \bar{\mathbf{u}}_2^S$ can be found to be

$$T = \frac{n^* \pi}{4\beta D} \frac{K^2 D^2 + (n^* \pi)^2}{KD}. \quad (4.5)$$

The existence of such a resonant Rossby-wave mode, which in linear theory exhibits unlimited gravity-wave-induced growth of \bar{q}_2^L , gives a clear example of an exception to the dissipation assumption in at least one case.

5. Generalized Lagrangian-mean theory

In the previous section the forcing of $\bar{\mathbf{u}}_2^L$ was described in terms of the Stokes drift $\bar{\mathbf{u}}_2^S$. It can be conjectured that the general non-dissipative effect studied, i.e. the permanent deformation of PV contours by gravity-wave-induced material particle displacements, is independent of the special characteristics of the shallow-water model. For instance, non-dissipating gravity waves in the standard Boussinesq model of stratified, three-dimensional flow are known to produce irreversible material displacements (e.g. Bretherton 1969).

However, in the Boussinesq model $\nabla \cdot \mathbf{u} \equiv 0$ and as a consequence the leading-order $\bar{\mathbf{u}}_2^S$ for vertically propagating monochromatic gravity waves is zero, a feature that is connected to the fact that a plane monochromatic gravity wave is a trivial exact solution of the Boussinesq equations (with or without background rotation), because particles move in planes of constant wave phase in this system. Monochromatic shallow-water gravity waves, on the other hand, are not exact solutions and have a non-zero leading-order Stokes drift. This leads us to suspect that the use of $\bar{\mathbf{u}}_2^S$ as the central quantity to describe the forcing of $\bar{\mathbf{u}}_2^L$ may be model-dependent, i.e. special to the shallow water model, and hence that the formulae derived in the previous section cannot be expected to simply carry over to other flow models.

In addition, the perturbative, small-amplitude approach of the previous section may be a poor guide to what is relevant in atmospheric or oceanographic flows that exhibit large wave amplitudes $a \sim 1$. Finite-amplitude counterparts of (3.35), should they exist, would be very helpful in discerning robust features of the established results that generalize to finite-amplitude waves. However, it is very difficult to manipulate the Eulerian-mean equations into a form that allows us to collect all the terms that contribute to the mean material velocity at orders beyond $O(a^2)$.

For both reasons, using GLM theory (AM78*a,b*) turns out to be decisively advantageous here. GLM theory establishes a nonlinear definition of $\bar{\mathbf{u}}^L$ at the outset and then derives general equations for its evolution from the equations of motion. The formalism of the theory applies for different forms of averaging, e.g. it applies for zonal averaging as well as for the slow-modulation average over the rapidly varying gravity-wave phase used in this paper. The physical interpretation of $\bar{\mathbf{u}}^L$ is dependent on the particular choice of averaging (see AM78*a* for an interpretation in the zonal-average case). In the special case of a slow-modulation average the physical interpretation is very simple: trajectories of $\bar{\mathbf{u}}^L$ (i.e. solutions of $d\mathbf{x}/dt = \bar{\mathbf{u}}^L(\mathbf{x}, t)$) are exactly the mean material particle trajectories sought. The mean-flow and Stokes-drift components of the motion of a material particle are combined in $\bar{\mathbf{u}}^L$, and the essential point is that $\bar{\mathbf{u}}^L$ only picks up that part of the material motion that is cumulative on average.

Two important vector fields $\boldsymbol{\xi}$ and \mathbf{p} emerge in GLM. The first generalizes to finite amplitude the linearized particle displacements $\boldsymbol{\xi}'$ used before. The second is a quantity called *pseudomomentum* (\mathbf{p} is strictly the pseudomomentum per unit mass, but here it will be loosely called pseudomomentum as well), whose curl will be seen to be the central quantity in the description of the forcing of $\nabla \times \bar{\mathbf{u}}^L$. Equation (3.35) involving the Stokes drift $\bar{\mathbf{u}}_2^S$ in the previous section will then appear as a simple special case by virtue of a near-equality of pseudomomentum and Stokes drift valid for slowly varying shallow-water gravity waves. It is, however, the pseudomomentum, and not the Stokes drift, that generalizes to stratified three-dimensional flow systems.

To prepare for this use of GLM theory it is necessary to establish some special notation and to give a brief outline of the kinematical workings of the theory. The

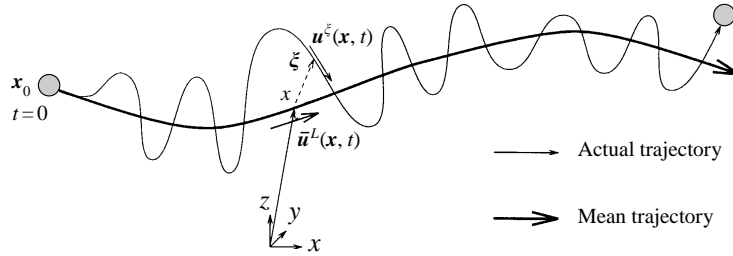


FIGURE 3. Mean and actual particle trajectories, which are supposed to have started from the same position \mathbf{x}_0 . The position $\mathbf{x} + \boldsymbol{\xi}(\mathbf{x}, t)$ is the *actual* position of the particle whose *mean* position is \mathbf{x} at time t .

theory is then applied to the shallow-water system, which produces a fully nonlinear GLM circulation theorem and a fully nonlinear GLM PV theorem. The $O(a^2)$, small-amplitude forms of these equations are then shown to be the same as the $O(a^2)$ equations (3.35) and (3.38) derived previously. Section 9 shows how the same GLM formalism can be applied to the Boussinesq model of stratified, three-dimensional flow. We shall need only slow-modulation averaging, and so the kinematics is described in terms of it; see AM78*a, b* for a full account of GLM theory.

5.1. Slow-modulation GLM theory

Consider the trajectory (i.e. solution of $d\mathbf{x}/dt = \mathbf{u}(\mathbf{x}, t)$) of a material particle starting at point \mathbf{x}_0 in figure 3. The picture suggests that the motion of the particle is such that it can be decomposed into a slow and a fast part by averaging over the fast timescale. This averaging process associates two different trajectories with each particle: first its actual, rapidly varying trajectory (thin line in figure 3), and second its mean, slowly varying trajectory (bold line in figure 3). GLM theory now postulates the existence of a unique disturbance-associated particle displacement field $\boldsymbol{\xi}(\mathbf{x}, t)$ that links these two trajectories (dashed arrow in figure 3). The field $\boldsymbol{\xi}(\mathbf{x}, t)$ depends on the fast timescale, and is defined such that

$$\mathbf{x} + \boldsymbol{\xi}(\mathbf{x}, t) \quad (5.1)$$

is the *actual* position of the particle whose *mean* position is \mathbf{x} at time t . The sense in which \mathbf{x} is the mean position is defined by

$$\overline{\boldsymbol{\xi}(\mathbf{x}, t)} = 0, \quad (5.2)$$

where the overbar denotes the slow-modulation average over the fast timescale.† Note that the particle whose *mean* position is \mathbf{x} at time t is not, in general, the same as the particle that is *at* \mathbf{x} at time t . In essence, GLM theory treats ordinary space (i.e. all the points \mathbf{x} in the domain) as a time-dependent reference space for both mean and actual trajectories. The first reference is established by the trivial map $\mathbf{x} \rightarrow \mathbf{x}$, which associates with \mathbf{x} the mean trajectory that touches \mathbf{x} at time t . The second reference is established by $\mathbf{x} \rightarrow \mathbf{x} + \boldsymbol{\xi}(\mathbf{x}, t)$ (i.e. (5.1)), which associates with \mathbf{x} the

† For (5.1) to work satisfactorily one has to assume that each point \mathbf{x} is touched by exactly one mean trajectory at a given time t , because otherwise $\boldsymbol{\xi}(\mathbf{x}, t)$ would not be unique. In other words, mean particle trajectories must not cross each other. It is not *a priori* clear whether or not this will occur. Distinct material particles may share the same mean position. Despite these cautionary remarks the possible crossing of mean trajectories will now be assumed not to occur, and the map in (5.1) will be assumed to be a single-valued function.

actual particle trajectory of the same particle. This dual reference avoids the use of classical Lagrangian particle labels as a reference space.

An exact Lagrangian-mean velocity can now be defined as

$$\bar{\mathbf{u}}^L(\mathbf{x}, t) \equiv \overline{\mathbf{u}(\mathbf{x} + \boldsymbol{\xi}(\mathbf{x}, t), t)}, \quad (5.3)$$

which is the finite-amplitude counterpart of $\bar{\mathbf{u}}_2^L$ of the previous section. By definition, $\bar{\mathbf{u}}^L$ is the mean velocity of the particle whose mean position is \mathbf{x} at time t . The important point is that the averaging is performed over the values of \mathbf{u} at the actual particle positions, see figure 3. Mean trajectories are defined as integral curves of $\bar{\mathbf{u}}^L(\mathbf{x}, t)$, and this leads naturally to the definition of the Lagrangian-mean time derivative

$$\bar{D}^L \equiv \frac{\partial}{\partial t} + \bar{\mathbf{u}}^L \cdot \nabla, \quad (5.4)$$

which is the derivative following mean trajectories.

The Lagrangian mean of any function ϕ is defined in analogy to (5.3). It is convenient to introduce a notation for ‘lifting’ a function ϕ from mean to actual particle positions,

$$\phi^\xi(\mathbf{x}, t) \equiv \phi(\mathbf{x} + \boldsymbol{\xi}(\mathbf{x}, t), t); \quad (5.5)$$

then $\bar{\phi}^L \equiv \overline{\phi^\xi(\mathbf{x}, t)}$. The difference between Lagrangian and Eulerian mean

$$\bar{\phi}^S \equiv \bar{\phi}^L - \bar{\phi} \quad (5.6)$$

is defined as the Stokes correction, or Stokes drift in the special case of velocity. The quantity $\phi^l \equiv \phi^\xi - \bar{\phi}^L$ defines the Lagrangian deviation from the average value of the field ϕ , following a particle. Two important properties of the rates of change of ϕ^ξ result from the chain rule of differentiation:

$$(\phi^\xi)_{,t} = (\phi_{,t})^\xi + (\phi_{,j})^\xi \xi_{j,t} \quad \text{and} \quad (\phi^\xi)_{,i} = (\phi_{,i})^\xi + (\phi_{,j})^\xi \xi_{j,i}, \quad (5.7)$$

where $(\)_{,t}$ denotes time-differentiation, $(\)_{,i}$ denotes covariant differentiation with respect to x_i , the ξ_j are the components of $\boldsymbol{\xi}$, and summation over repeated indices is understood.

By definition, (5.1) evaluated along a mean trajectory $\mathbf{x}(t)$ traces out the actual trajectory of the particle whose mean trajectory $\mathbf{x}(t)$ is being followed. Therefore the time derivative \bar{D}^L of (5.1) along a mean trajectory is equal to $\mathbf{u}^\xi(\mathbf{x}, t)$, the actual particle velocity, and this yields the evolution equation for $\boldsymbol{\xi}$ as

$$\mathbf{u}^\xi = \bar{D}^L(\mathbf{x} + \boldsymbol{\xi}) = \bar{\mathbf{u}}^L + \bar{D}^L \boldsymbol{\xi} \quad \Rightarrow \quad \bar{D}^L \boldsymbol{\xi} = \mathbf{u}^\xi - \bar{\mathbf{u}}^L \equiv \mathbf{u}^l. \quad (5.8)$$

Here $\mathbf{u}^l = \mathbf{u}^\xi - \bar{\mathbf{u}}^L$ is the Lagrangian disturbance velocity. Given $\mathbf{u}(\mathbf{x}, t)$ and initial conditions for $\boldsymbol{\xi}$ (which are $\boldsymbol{\xi}(\mathbf{x}, 0) = 0$ if, as is assumed here, there is no disturbance at $t = 0$) (5.3), (5.4), and (5.8) determine $\boldsymbol{\xi}$ and therefore $\bar{\mathbf{u}}^L$ at all later times.

A consequence of (5.7) and (5.8) is two important rules connecting material derivatives on mean and actual trajectories:

$$\bar{D}^L \phi^\xi = \left(\frac{D\phi}{Dt} \right)^\xi \quad \text{and} \quad \bar{D}^L \bar{\phi}^L = \overline{\left(\frac{D\phi}{Dt} \right)^L}. \quad (5.9)$$

The first rule is obtained by substituting (5.7) and (5.8) in its left-hand side and observing that $[\mathbf{u} \cdot \nabla \phi]^\xi = u_j^\xi (\phi_{,j})^\xi$, and the second is simply the average of the first. The simplicity of the Lagrangian mean of a material derivative is a major advantage of GLM theory.

A characteristic difference between standard Eulerian-mean theories and GLM theory – sometimes called the ‘divergence effect’ (AM78a, McIntyre 1988) – is that in GLM theory $\nabla \cdot \mathbf{u} = 0$ does not imply that $\nabla \cdot \bar{\mathbf{u}}^L = 0$. This divergence effect arises naturally in GLM theory owing to the interplay between Lagrangian averaging and the use of (5.2) to define mean particle positions. The significance of the divergence effect is further discussed in AM78a, where it is stressed that a mean density field satisfying the continuity equation

$$\bar{D}^L \bar{\rho} + \bar{\rho} \nabla \cdot \bar{\mathbf{u}}^L = 0 \quad (5.10)$$

will in general not be equal to $\bar{\rho}^L$. It proves convenient to use $\bar{\rho}$, as defined by (5.10) and a suitable initial condition, in GLM theory. If there are no disturbances initially, then $\bar{\rho}(\mathbf{x}, 0) = \rho(\mathbf{x}, 0)$. Furthermore, in this case $\bar{\rho} = \tilde{\rho}$, i.e. $\tilde{\rho}$ is a mean quantity, as can be shown by averaging (5.10) and noting that if $\tilde{\rho} = \bar{\rho}$ initially, then it holds at all later times (see AM78a for further discussion of this point).

In the same way as ordinary density measures the dilation or contraction of actual material volumes, $\tilde{\rho}$ measures the dilation or contraction of *mean* material volumes. It is straightforward to show (AM78a) that therefore $\tilde{\rho}$ is equal to ρ^ξ times the Jacobian of the ‘lifting’ map $\mathbf{x} \rightarrow \mathbf{x} + \boldsymbol{\xi}$, i.e.

$$\tilde{\rho} = \rho^\xi \frac{\partial(\mathbf{x} + \boldsymbol{\xi})}{\partial(\mathbf{x})}. \quad (5.11)$$

5.2. Shallow-water GLM theory

The GLM theory is now applied to the two-dimensional shallow-water equations (cf. (2.2), (2.3)). There is, however, a problem in that the standard, fully nonlinear GLM theory (i.e. theorem I and its corollaries in AM78a) applies only for constant Coriolis parameter, i.e. $\beta = 0$. The root of the problem is that $\overline{(\mathbf{f}\hat{\mathbf{z}} \times \mathbf{u})}^L \neq \mathbf{f}\hat{\mathbf{z}} \times \bar{\mathbf{u}}^L$ if $\beta \neq 0$, and in an exact theory this necessitates a non-trivial modification of the standard GLM definition of pseudomomentum \mathbf{p} in (5.16) below. Although this can be done in principle (Bühler 1996), for simplicity the fully nonlinear GLM theory is here only applied to (2.2) with $\beta = 0$. Section 5.3 below analyses the small-amplitude limit of the GLM equations, and it is shown there how $\beta \neq 0$ can be incorporated in that limit.

Following (5.10) and (5.11), the continuity equation (2.3) is replaced by two equivalent equations for \tilde{h} :

$$\bar{D}^L \tilde{h} + \tilde{h} \nabla \cdot \bar{\mathbf{u}}^L = 0, \quad (5.12)$$

$$\tilde{h} = h^\xi \frac{\partial(x + \xi, y + \eta)}{\partial(x, y)} = h^\xi \left(1 + \nabla \cdot \boldsymbol{\xi} + \frac{\partial(\xi, \eta)}{\partial(x, y)} \right), \quad (5.13)$$

where (ξ, η) are the two components of $\boldsymbol{\xi}$. In the momentum equation (2.2) it proves advantageous to preserve the gradient character of the pressure term, and (5.7) indicates how this can be achieved:

$$(h_{,j})^\xi (\delta_{ji} + \xi_{j,i}) = (h^\xi)_{,i}. \quad (5.14)$$

Therefore (2.2) is first ‘lifted’ to actual particle positions (i.e. each term is evaluated at $\mathbf{x} + \boldsymbol{\xi}(\mathbf{x}, t)$), then multiplied with $\delta_{ji} + \xi_{j,i}$, and finally averaged over the fast timescale. The result is a special case of theorem I of AM78a, namely

$$\bar{D}^L (\bar{u}_i^L - \mathbf{p}_i) + \bar{u}_{k,i}^L (\bar{u}_k^L - \mathbf{p}_k) + [f_0 \hat{\mathbf{z}} \times \bar{\mathbf{u}}^L]_i + c_0^2 \bar{h}_{,i}^L = \frac{1}{2} \left(\overline{u_j^\xi [u_j^\xi + (f_0 \hat{\mathbf{z}} \times \boldsymbol{\xi})_j]} \right)_{,i}, \quad (5.15)$$

where

$$\mathbf{p}_i \equiv - \overline{\left([\mathbf{u}^l + \frac{1}{2}f_0\hat{\mathbf{z}} \times \boldsymbol{\xi}]_j \xi_{j,i} \right)} \quad (5.16)$$

is the GLM definition of the pseudomomentum (per unit mass) \mathbf{p} .

Like $\bar{\mathbf{u}}^S$, \mathbf{p} is a wave property in the sense that its leading-order expression is $O(a^2)$, and that it can be consistently computed from linear wave solutions alone. Pseudomomentum usually appears in studies of flow situations in which the mean flow exhibits a translational symmetry, which leads to global conservation of the component of $\tilde{h}\mathbf{p}$ parallel to the symmetry direction (AM78*b*; Shepherd 1990). It turns out, however, that \mathbf{p} plays an essential role in mean-flow forcing *regardless* of whether individual components of it are conserved or not. This becomes apparent when the curl of (5.15) is taken:

$$\begin{aligned} \bar{D}^L [\nabla \times (\bar{\mathbf{u}}^L - \mathbf{p}) + f_0] + [\nabla \times (\bar{\mathbf{u}}^L - \mathbf{p}) + f_0] \nabla \cdot \bar{\mathbf{u}}^L &= 0 \\ \Leftrightarrow \boxed{\bar{D}^L \tilde{q} = 0 \quad \text{for} \quad \tilde{q} \equiv \frac{[\nabla \times (\bar{\mathbf{u}}^L - \mathbf{p}) + f_0]}{\tilde{h}}} &, \quad (5.17) \end{aligned}$$

where the last line makes use of (5.12).[†] It is remarkable that only $\nabla \times \mathbf{p}$ enters but not the symmetric part of the gradient of \mathbf{p} , which is a repercussion of the peculiar term $-\bar{u}_{k,i}^L \mathbf{p}_k$ in the momentum equation. Furthermore, it should be noted that (5.17) holds for arbitrary structure of the disturbance, i.e., in contrast with the previous section, it has not been assumed here that the disturbance is a slowly varying wavetrain.

Before going on it should be noted that, to the extent that \mathbf{p} can be regarded as given, (5.17) can be directly exploited as an equation for the vortical part of $\bar{\mathbf{u}}^L$ forced by the curl of \mathbf{p} . At small wave amplitude this must work because \mathbf{p} is a wave property. At large wave amplitude (5.17) still holds, but now the back-effect of $\bar{\mathbf{u}}^L$ onto \mathbf{p} can no longer be neglected and hence \mathbf{p} can no longer be regarded as given. Note that equation (5.17) gives no information about $\nabla \cdot \bar{\mathbf{u}}^L$ and hence the negligibility of the divergence part of $\bar{\mathbf{u}}^L$ (and therefore of variations in \tilde{h} in (5.17) as well) has to be either assumed here or to be established by a fuller analysis of (5.15), as was done in the previous sections.

Equation (5.17) is the finite-amplitude counterpart (for $\beta = 0$) of (3.36) and (3.37), with \mathbf{p} replacing the Stokes drift. The Lagrangian-mean potential vorticity \bar{q}^L is itself invariant on mean trajectories by (5.9), and if there has been no disturbance initially, and therefore $\tilde{q} = \bar{q}^L$ at the initial time, then the invariant quantity in (5.17) is equal to \bar{q}^L at all times. This gives the finite-amplitude counterpart of (3.38), i.e.

$$\boxed{\bar{q}^L = \tilde{q} = \frac{[\nabla \times (\bar{\mathbf{u}}^L - \mathbf{p}) + f_0]}{\tilde{h}}} \quad (5.18)$$

The equality of \tilde{q} and \bar{q}^L subject to non-dissipative evolution and to suitable initialization has been noted before by AM78*a* and others. However, it seems that rather more can be said. Specifically, we have the following lemma.

[†] The concurrence of $1/h$ and $1/\tilde{h}$ in (1.1) and (5.17) is accidental; if two-dimensional *incompressible* flow were studied then (1.1) would hold without the factor $1/h$, but $1/\tilde{h}$ would still have to be retained in (5.17). This is a consequence of $\nabla \cdot \mathbf{u} = 0$ not implying $\nabla \cdot \bar{\mathbf{u}}^L = 0$.

LEMMA. *The equality (5.18) on a mean material trajectory holds subject only to suitable initialization, which is understood to mean that $\tilde{q} = \bar{q}^L$ and that \tilde{h} is a mean quantity fulfilling (5.13) at one point of the mean material trajectory. This can be achieved, for instance, by initializing the flow without any disturbance. The equality (5.18) then holds regardless of the presence of an arbitrary body force, of dissipative origin or otherwise, in the momentum equation. In other words, although in the presence of forcing or dissipation neither \tilde{q} nor \bar{q}^L will be invariant on mean material trajectories, they will, subject only to the suitable initialization, change in exactly the same way together.*

Two alternative proofs of this lemma are possible. For the first proof consider the shallow-water momentum equation (2.2) with an arbitrary force \mathbf{F} on the right-hand side. It is then straightforward to show that the evolution equations for q , \bar{q}^L , and \tilde{q} are, respectively,

$$\frac{Dq}{Dt} = \frac{\nabla \times \mathbf{F}}{h}, \quad \overline{D^L \bar{q}^L} = \overline{\left[\frac{(\nabla \times \mathbf{F})^\xi}{h^\xi} \right]}, \quad \overline{D^L \tilde{q}} = \frac{\epsilon_{ki} \left[F_j^\xi (\delta_{ji} + \xi_{j,i}) \right]_{,k}}{\tilde{h}}, \quad (5.19)$$

where $\epsilon_{ki} = -\epsilon_{ik}$ is the two-dimensional alternating symbol such that $\epsilon_{12} = 1$. Using (5.13), i.e. the relation between \tilde{h} and h^ξ that depends on the initialization, and the chain rule (5.7) then establishes, after some manipulation, the exact equality of the two mean right-hand sides in (5.19), which completes this proof.

A second proof uses the connection between PV and the circulation around material contours, which stresses the kinematical character of the lemma, and which also clarifies the origin of the definition of \mathbf{p} in (5.16). Consider two closed contours C and C^ξ , where C^ξ is the image of C under the lifting map $\mathbf{x} \rightarrow \mathbf{x} + \boldsymbol{\xi}$, as illustrated in figure 4. Note that there is no simple relation between the shapes or enclosed areas of the two contours. The circulation Γ around the contour C^ξ is defined in the usual way, but Γ can also be related to an integral around C using the lifting map. This gives

$$\begin{aligned} \Gamma &\equiv \oint_{C^\xi} [\mathbf{u} + \frac{1}{2} f_0 \hat{\mathbf{z}} \times \mathbf{x}] \cdot d\mathbf{x} = \oint_C [\mathbf{u}^\xi + \frac{1}{2} f_0 \hat{\mathbf{z}} \times \mathbf{x}^\xi] \cdot d\mathbf{x}^\xi \\ &= \oint_C [\mathbf{u}^\xi + \frac{1}{2} f_0 \hat{\mathbf{z}} \times \mathbf{x}^\xi]_i (\delta_{ij} + \xi_{i,j}) dx_j, \end{aligned} \quad (5.20)$$

which uses

$$d\mathbf{x}^\xi = d(\mathbf{x} + \boldsymbol{\xi}) = d\mathbf{x} + (d\mathbf{x} \cdot \nabla) \boldsymbol{\xi}.$$

Averaging this expression affects only the integrand because C is a mean contour, and this defines a particular mean circulation $\tilde{\Gamma}$ as

$$\tilde{\Gamma} \equiv \overline{(\Gamma)} = \oint_C [\bar{\mathbf{u}}^L - \mathbf{p} + \frac{1}{2} f_0 \hat{\mathbf{z}} \times \mathbf{x}] \cdot d\mathbf{x}, \quad (5.21)$$

after using the definition of \mathbf{p} in (5.16).

On the other hand, Γ can be rewritten using Stokes' theorem as

$$\Gamma = \int_A \int_{A^\xi} (\nabla \times \mathbf{u} + f_0) dx dy = \int_A \int_{A^\xi} qh dx dy = \iint_A q^\xi (h dx dy)^\xi \quad (5.22)$$

$$= \iint_A q^\xi \tilde{h} dx dy, \quad (5.23)$$

where A and A^ξ denote the areas enclosed by C and C^ξ , respectively, and where (5.13)

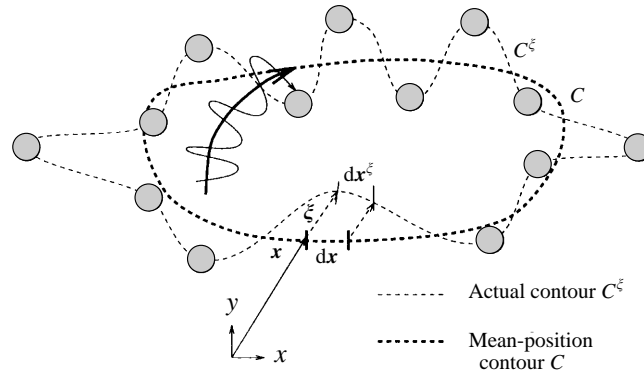


FIGURE 4. Actual material contour C^ξ and mean material contour C . Particles on the actual contour have mean positions on the mean contour. Also depicted are the mean and actual trajectories of one particular particle.

has been used in the last step. Averaging the last expression then gives

$$\overline{(\Gamma)} = \iint_A \bar{q}^L \tilde{h} \, dx dy. \tag{5.24}$$

Similarly, using Stokes's theorem in (5.21) together with the definition of \tilde{q} in (5.17) gives

$$\tilde{\Gamma} = \iint_A (\nabla \times (\bar{\mathbf{u}}^L - \mathbf{p}) + f_0) \, dx dy = \iint_A \tilde{q} \tilde{h} \, dx dy. \tag{5.25}$$

Finally, as $\tilde{\Gamma} = \overline{(\Gamma)}$ must hold for arbitrary choice of A , (5.24) and (5.25) imply that $\tilde{q} = \bar{q}^L$, which completes this second proof.

5.3. Small-amplitude shallow-water beta-channel

The GLM PV equation (5.17) is now evaluated in the small-amplitude limit, and at the same time $\beta \neq 0$ is incorporated. Adding the β -term to the Coriolis parameter adds the terms

$$\begin{aligned} \overline{[\beta y \hat{\mathbf{z}} \times \mathbf{u}]_j^\xi (\delta_{ji} + \xi_{j,i})} &= \beta \epsilon_{j3n} \overline{(y + \eta) u_n^\xi (\delta_{ji} + \xi_{j,i})} \\ &= \beta \epsilon_{j3n} \left\{ y \left(\overline{u_n^L} \delta_{ji} + \overline{u_n^L \xi_{j,i}} \right) + \overline{\eta u_n^L} \delta_{ji} + \overline{\eta u_n^\xi \xi_{j,i}} \right\} \end{aligned} \tag{5.26}$$

to the left-hand side of (5.15). This uses $\overline{\mathbf{u}^\xi \xi} = \overline{(\bar{\mathbf{u}}^L + \mathbf{u}^L) \xi} = \overline{\mathbf{u}^L \xi}$.

The leading-order expressions for the various GLM fields are (cf. AM78a)

$$\bar{\mathbf{u}}^L = \mathbf{U} + \bar{\mathbf{u}}_2^L + O(a^3), \tag{5.27}$$

$$\bar{\mathbf{u}}_2^L - \bar{\mathbf{u}}_2 = \bar{\mathbf{u}}_2^S = (\xi' \cdot \nabla) \mathbf{u}'_1 + \frac{1}{2} \overline{\xi'_i \xi'_j} U_{,ij} + O(a^3), \tag{5.28}$$

$$\mathbf{u}^L \equiv \mathbf{u}^\xi - \bar{\mathbf{u}}^L = \mathbf{u}'_1 + (\xi' \cdot \nabla) \mathbf{U} + O(a^2) \approx \mathbf{u}'_1, \tag{5.29}$$

$$D_i \xi'_i = \mathbf{u}'_1 + (\xi' \cdot \nabla) \mathbf{U} + O(a^2) \approx \mathbf{u}'_1, \tag{5.30}$$

where the approximate equalities come from the negligibility of gradients of \mathbf{U} on the scale of the gravity waves. Consider only contributions at $O(a^2)$ now. Using the above relations the scale of the two terms in round brackets in (5.26) is estimated as $O(\beta L a^2 c_0)$, whereas the other terms are estimated to be much smaller. The first term

adds naturally to the existing Coriolis force in (5.15), i.e. at $O(a^2)$

$$[f_0 \hat{\mathbf{z}} \times \bar{\mathbf{u}}_2^L]_i \rightarrow [(f_0 + \beta y) \hat{\mathbf{z}} \times \bar{\mathbf{u}}_2^L]_i \quad (5.31)$$

in (5.15). The second term in round brackets in (5.26) is in fact *not* $O(\beta L a^2 c_0)$. This is because of the cross-product between the $O(a)$ wave fields in it, which vanishes in the limit of a plane gravity wave. Hence the second term is smaller than the dominant scale by a factor of at least κL . Therefore the change (5.31) is the only leading-order change that needs to be made when adapting (5.15) for the $O(a^2)$ β -plane limit. In particular, the pseudomomentum definition (5.16) remains unchanged to leading order, in accordance with the fact that the β -effect is negligible for the small-scale gravity waves.

The leading-order Stokes drift is found from (5.28) as

$$\bar{\mathbf{u}}_2^S = \overline{(\boldsymbol{\xi}' \cdot \nabla) \mathbf{u}'_1} + \frac{1}{2} \overline{\eta'^2} U_{yy} \hat{\mathbf{x}} = \bar{h}'_1 \mathbf{u}'_1 + O(\mu a^2 c_0) + O(\mu^2 a^2 \mathcal{U}), \quad (5.32)$$

where (3.8) has been used. This shows that the leading-order GLM definition of $\bar{\mathbf{u}}^S$ is consistent with the $O(a^2)$ Eulerian definition in (3.16). Therefore

$$\bar{\mathbf{u}}^L = \bar{\mathbf{u}} + \bar{\mathbf{u}}^S = U \hat{\mathbf{x}} + \bar{\mathbf{u}}_2^L + O(a^3) \quad (5.33)$$

can be used in (5.17). The leading-order pseudomomentum \mathbf{p}_2 for slowly varying waves has the generic form (cf. AM78*a, b*)

$$\mathbf{p}_2 = \frac{\mathbf{k}}{\bar{\omega}} E, \quad (5.34)$$

and comparison with (3.17) shows that $\bar{\mathbf{u}}_2^S = \mathbf{p}_2$ here. This leading-order equality is special, valid for shallow-water gravity waves, but not valid more generally. In the Boussinesq system, as noted before, $\bar{\mathbf{u}}_2^S = 0$ for gravity waves, but \mathbf{p}_2 is still given by (5.34).

The $O(1)$ part of $\bar{\mathbf{D}}^L$ is equal to D_t , and comparing (3.28) and (5.12) then shows that \bar{h}_2 and \bar{h}'_2 satisfy the same equation, and hence $\bar{h}_2 = \bar{h}'_2$ if the flow is initialized without disturbance. This equality, which can also be proven directly by averaging (5.13) and noting that the Jacobian term vanishes for plane shallow-water gravity waves, is again special, and does not generalize to other systems. Two-dimensional surface gravity waves, for instance, provide an example in which the Eulerian mean density and the corresponding $\bar{\rho}$ differ at leading order (McIntyre 1988). It can be noted in passing that from (5.13) and (3.8) it also follows that

$$\bar{h}_2^L = \bar{h}_2 + \bar{h}'_1{}^2 \Leftrightarrow \bar{h}_2^S = \bar{h}'_1{}^2 \quad (5.35)$$

to leading order.

One can now evaluate (5.17) at leading order. The derivation leading from (5.15) to (5.17) is affected only by the additional term in (5.31). This term, however, only adds βy to the background vorticity. Therefore (5.17) at $O(a^2)$ is (neglecting changes in \bar{h}_2 as before)

$$D_t \nabla \times \bar{\mathbf{u}}_2^L + (\beta - U_{yy}) \bar{v}_2^L = D_t \nabla \times \mathbf{p}_2 = D_t \nabla \times \bar{\mathbf{u}}_2^S, \quad (5.36)$$

where use has been made of the fact that $\bar{\mathbf{D}}^L = D_t + (\bar{\mathbf{u}}_2^L \cdot \nabla)$ to $O(a^2)$. This is equal to the $O(a^2)$ mean vorticity equation (3.35) of the previous section, which is a useful check on the validity of (3.35) as it has now been derived via two independent routes.

6. Extension of the parameter regime and modified shallow-water model

The previously made convenient assumption $L/L_R \ll 1$ led to the simplest possible mean-flow response problem, but this assumption was not based on any particular features of realistic atmospheric or oceanic motions. This suggests a natural extension of the parameter regime by relaxing the restriction $L/L_R \ll 1$ now, i.e. by allowing the parameter ϵ in table 1 to take any value, including values much greater than unity. It turns out that in this new regime significant stretching of background vorticity by \bar{h}_2 can take place, which then needs to be taken into account in (3.29) and other equations to calculate $\bar{\mathbf{u}}_2^L$. Furthermore, if $L/L_R \gg 1$ then it is possible that the wavelength of the gravity waves is itself comparable to L_R whilst remaining small compared to L . The gravity waves then become dispersive inertia–gravity waves, which feel both gravitational and Coriolis forces, and the associated changes in the wave structure need to be taken carefully into account.

In addition, a certain nonlinear modification of the pressure term in the shallow-water momentum equation is now considered. This artificial modification of the shallow-water model allows the dependence of the interaction effects on subtle changes in the details of the ‘elastic’ properties of the fluid to be discerned. Furthermore, it will be seen in §8 that such a modification is essential in order to arrive at a well-posed numerical simulation. Specifically, the modification is

$$c_0^2 \nabla h \quad \longrightarrow \quad \frac{c_0^2}{\gamma - 1} \nabla (h^{\gamma-1}), \tag{6.1}$$

where γ is a constant parameter not equal to one, but otherwise arbitrary (Bühler 1997). The form of (6.1) is motivated by the gas-dynamical analogy in which standard shallow-water flow is equivalent to two-dimensional flow of a homentropic perfect gas with ratio of specific heats $\gamma = 2$, and in which gravity waves correspond to sound waves. Of particular interest for the numerical simulations in §8 will be the modified model corresponding to $\gamma = -1$. Clearly, for arbitrary γ the equations of motion linearized around a background state with $h = 1$ remain unchanged, and therefore the gravity-wave structure does not depend on γ . Furthermore, as the gradient character of the pressure term is retained, the vorticity equation and the form and material invariance of PV also remain unchanged. The only dependence on γ therefore will occur in the $O(a^2)$ divergence equation (3.30).

The scaling in table 1 already includes a tighter bound on the size of U and β to ensure that the background flow in geostrophic balance continues to require only negligible deviations from unity of the background depth field. Also, the $O(a)$ gravity-wave structure in §2 has already allowed for low-frequency, inertia–gravity waves. The relation $\bar{\mathbf{u}}_2^S = \mathbf{p}_2$ still holds for slowly varying inertia–gravity wavetrains, by virtue of the robust relation $\mathbf{p}_2 = E \mathbf{k} / \hat{\omega}$ in that limit (AM78*b*), and the use of \mathbf{p}_2 instead of $\bar{\mathbf{u}}_2^S$ is preferred below.

The mean continuity and vorticity equations (3.28) and (3.29) are unchanged, except for the trivial substitution of \mathbf{p}_2 for $\bar{\mathbf{u}}_2^S$ in (3.29), i.e.

$$\boxed{D_t [\nabla \times \bar{\mathbf{u}}_2^L - (f - U_y) \bar{h}_2] + \bar{v}_2^L (\beta - U_{yy}) = D_t \nabla \times \mathbf{p}_2}. \tag{6.2}$$

The definition of \bar{q} in (3.36) needs to be amended by the term $-(f - U_y) \bar{h}_2$. The mean divergence equation (3.30) is changed in two places. On the left-hand side

$$c_0^2 \nabla^2 \bar{h}_2 \quad \longrightarrow \quad c_0^2 \nabla^2 \left(\bar{h}_2 + \frac{\gamma - 2}{2} \left(1 - \frac{f_0^2}{\hat{\omega}^2} \right) \frac{E}{c_0^2} \right), \tag{6.3}$$

and on the right-hand side

$$-\nabla^2 E/2 \longrightarrow -\left(1 + \frac{f_0^2}{\hat{\omega}^2}\right) \nabla^2 E/2. \quad (6.4)$$

These changes are consequences of the changed $O(a^2)$ pressure term and the changed gravity-wave structure, respectively. Using (3.15), the simplified divergence equation (3.33) can then be written as

$$\left(\frac{\partial^2}{\partial t^2} - c_0^2 \nabla^2\right) \bar{h}_2 + f_0 \nabla \times \bar{\mathbf{u}}_2^L = \left(\frac{\partial^2}{\partial t^2} + c_0^2 A \nabla^2\right) \frac{E}{c_0^2}, \quad (6.5)$$

where the constant A is defined as

$$A \equiv \frac{\gamma - 2}{2} \left(1 - \frac{f_0^2}{\hat{\omega}^2}\right) + \frac{1}{2} \left(1 + \frac{f_0^2}{\hat{\omega}^2}\right). \quad (6.6)$$

It is clear from (6.5) that the evolution of \bar{h}_2 will depend on the value of A , and that this dependence will manifest itself even when the wave field is steady. The scaling arguments advanced earlier, which allowed the neglect of \bar{h}_2 , are not valid here. For instance, during wave-field transience (6.2) is approximately replaced by (cf. (4.1))

$$\frac{\partial}{\partial t} [\nabla \times \bar{\mathbf{u}}_2^L - f_0 \bar{h}_2] = \frac{\partial}{\partial t} \nabla \times \mathbf{p}_2, \quad (6.7)$$

in which the relative size of the two terms in the square bracket now depends non-trivially on the value of ϵ and on the solution of (6.5).

As before, it is possible to use $\nabla \cdot \bar{\mathbf{u}}_2^L = 0$ at all times without making an appreciable error in the mean material displacements. For a steady wave field (6.5) becomes

$$\boxed{-c_0^2 \nabla^2 \bar{h}_2 + f_0 \nabla \times \bar{\mathbf{u}}_2^L = A \nabla^2 E}, \quad (6.8)$$

and the balanced evolution of the $O(a^2)$ mean flow is then described by (6.2) and (6.8) together with the constraint $\nabla \cdot \bar{\mathbf{u}}_2^L = 0$. Introducing a stream function Ψ^L such that $\bar{u}_2^L = -\Psi_y^L$ and $\bar{v}_2^L = \Psi_x^L$ allows (6.8) to be solved as

$$c_0^2 \bar{h}_2 = f_0 \Psi^L - AE \quad (6.9)$$

up to a harmonic function to be determined by boundary conditions. For definiteness the constant part of Ψ^L is fixed such that the total integral of Ψ^L over the channel is always zero. The boundary condition for Ψ^L at the walls is $\bar{v}_2^L = \Psi_x^L = 0$, and likewise a condition for $\partial \bar{h}_2 / \partial y$ must hold at the walls that maintains the vanishing of \bar{v}_2^L there. It turns out (see the Appendix) that away from the wall undulations (6.9) already implies this boundary condition, but that this is not so at the wall undulations, where a more complicated condition holds. However, (6.9) is still useful as a far-field approximation, valid at distances away from the walls not small compared to the zonal envelope scale of the gravity waves.†

Substituting (6.9) into (6.2), and using $(f - U_y) \bar{h}_2 \approx f_0 \bar{h}_2$, reduces the balanced system to a single equation for Ψ^L , namely

$$\boxed{D_t \left[\left(\nabla^2 - \frac{1}{L_R^2} \right) \Psi^L \right] + \frac{\partial \Psi^L}{\partial x} (\beta - U_{yy}) = D_t \left[\nabla \times \mathbf{p}_2 - \frac{A(\gamma, f_0/\hat{\omega})}{c_0 L_R} E \right]}, \quad (6.10)$$

† This influence of the boundary conditions explains the very special features of genuinely one-dimensional wave problems, in which the zonal wave envelope is effectively infinite and no far-field region exists (e.g. McIntyre 1981; Yih 1997, and the Appendix).

where the dependence of A on γ and the gravity-wave frequency has been highlighted. Equation (6.10) is the required generalization of (3.35).

For completeness, it can be noted that the finite-amplitude GLM results in §5 are affected by the extensions considered here only through a change

$$\bar{h}^L \rightarrow \overline{h^{(\gamma-1)}}^L / (\gamma - 1) \quad (6.11)$$

in the irrotational pressure term in (5.15). This change does not change the GLM vorticity equation.

Relaxing the restriction $L/L_R \ll 1$ is seen to have two quite different effects on the balanced mean-flow response. First, the structure of the balanced mean flow is modified in the usual quasi-geostrophic way to accommodate the finite Rossby deformation length L_R . Second, a new forcing term appears in the balanced equations, which induces a fundamentally different balanced mean-flow response to the previously studied response induced by the $\nabla \times \mathbf{p}_2$ term. However, this new forcing term, which is connected with \bar{h}_2 and E , – and related to classic ideas on acoustic ‘radiation stress’ (e.g. Brillouin 1925, 1936, 1964 ; AM78*a*; McIntyre 1981 and references therein) – turns out to be dependent on subtle model details such as the value of γ , the frequency of the gravity waves, and also on the details of the $O(a^2)$ wall boundary conditions. By contrast, the $\nabla \times \mathbf{p}_2$ term does not depend on any of these details.

This strengthens the impression that the mean-flow forcing connected with $\nabla \times \mathbf{p}_2$ is the most robust, model-independent part of the interaction problem studied. A corroboration of this view is found for at least one other standard flow model by the analysis of the three-dimensional Boussinesq system in §9, where it is shown that only $\nabla \times \mathbf{p}_2$, but not E , enters the mean-flow forcing in that model.

The simplest example of qualitatively new mean-flow features due to the new forcing term, which is also investigated numerically in §8, is given by the balanced flow just after spin-up of the waves in the extreme case that $L/L_R \gg 1$. This limit can be achieved without changing \mathbf{p}_2 or E , and hence the terms with coefficients $1/L_R$ must eventually dominate in (6.10). Therefore

$$\Psi^L \approx \frac{AL_R}{c_0} E = \frac{A}{f_0} E \quad (6.12)$$

sufficiently far from the walls. This implies a strikingly different streamline pattern to that shown in figure 2. The pattern in figure 2 shows a near-equality of $\bar{\mathbf{u}}_2^L$ and \mathbf{p}_2 (or $\bar{\mathbf{u}}_2^S$) in the centre of the channel, with velocity maxima in the core of the wavetrains, compatible with simple ideas about the waves’ Stokes drift ‘dragging’ the fluid with it. The response according to (6.12), on the other hand, implies completely different patterns of $\bar{\mathbf{u}}_2^L$ and \mathbf{p}_2 , with velocity maxima located at the flanks of the cores, where ∇E is largest (cf. §8 for a numerical simulation). On the other hand, in the core, where \mathbf{p}_2 is largest, $\bar{\mathbf{u}}_2^L$ is now zero.

7. Dissipative and non-dissipative gravity-wave effects

As noted in the introduction, dissipative effects are naturally represented in the prognostic step of the PV evolution, changing the value of PV along material trajectories. These wave-induced dissipative changes to the PV can in many cases be neatly summarized by the so-called ‘pseudomomentum rule’ (e.g. McIntyre & Norton 1990, and references therein). In the shallow-water model this rule simply states that dissipative wave-induced PV changes are equal to those that would arise if (a) the gravity waves were absent, and (b) there were instead an effective mean force per unit

mass acting in the direction of the waves' pseudomomentum, and equalling in strength the local dissipation rate of pseudomomentum per unit mass. Using this concept of an effective mean force is convenient, for instance, for the purpose of gravity-wave parametrizations in numerical models working with momentum equations, in which such a force can easily be incorporated.

The robust equality between \bar{q} , which in this paper is the central quantity in a diagnostic step that takes gravity waves into account, and \bar{q}^L , which is the central quantity in a dissipative prognostic step using the pseudomomentum rule, suggests that both dissipative and non-dissipative effects can be simply combined. The standard quasi-geostrophic system, when augmented with leading-order gravity-wave terms according to (1.3) and the pseudomomentum rule, would then appear as

$$\left(\nabla^2 - \frac{1}{L_R^2}\right) \Psi = q - q_0 + \nabla \times \mathbf{p}_2 - \frac{A}{c_0 L_R} E, \quad (7.1)$$

$$\mathbf{u} = \hat{\mathbf{z}} \times \nabla \Psi, \quad (7.2)$$

$$\left(\frac{\partial}{\partial t} + \mathbf{u} \cdot \nabla\right) q = \frac{1}{\tau} \nabla \times \mathbf{p}_2, \quad (7.3)$$

where q_0 is the background PV (e.g. equal to $f - U_y$ as before), and τ is a dissipation timescale such that E/τ is equal to the dissipated wave energy per unit time and unit mass. The first two equations together form the diagnostic inversion step, (7.3) is the prognostic evolution step, and \mathbf{p}_2 , τ and E are given, for instance, by a suitable ray-tracing algorithm that includes dissipative effects. This model neglects Stokes corrections in the PV and tacitly uses the Lagrangian-mean velocity as its velocity field.

It can be noted that the effects due to dissipating gravity waves go together with the familiar weakening of the waves' pseudomomentum, as is built into the pseudomomentum rule in (7.3). However, this weakening of the waves' pseudomomentum is absent in the leading-order approximation to the non-dissipative effects. This makes it appear unlikely that ways could be found in which the non-dissipative effects could be captured in the usual, dissipative framework that relates mean-flow forcing to the flux divergence of a suitable wave activity, as is often the case for zonally symmetric mean flows (e.g. Andrews *et al.* 1987).

8. Numerical simulations

Numerical simulations are performed to verify the results of the small-amplitude theory, and as a first step towards extending the study to large-amplitude gravity waves. However, it turns out that the standard shallow-water (SSW) model is not useful for a study that requires slowly varying, non-dissipating trains of gravity waves containing many individual wavelengths. This is because of the well-known nonlinear steepening and concomitant shock formation of SSW gravity waves, which disrupts a straightforward integration of the equations, and leads to spurious oscillations, strong numerical dissipation, and essentially uncontrollable growth of small-scale noise unless highly specialized, shock-permitting numerical techniques are used. The time for shocks to form is inversely proportional to the wave amplitude a , and generally very short. For instance, a SSW gravity wave with moderate amplitude $a = 0.1$ will break after just one wavelength of propagation. Clearly, this shock formation did not pose a problem for the asymptotic small-amplitude theory of the previous sections, because for any finite number of wavelengths needed to cross the

channel the value of a can always be chosen sufficiently small to make the nonlinear steepening negligible.

It can be argued (Bühler 1997) that self-induced shock formation of the kind observed in the SSW system, although typical for longitudinal compressible waves such as sound waves, is not typical for transverse incompressible waves such as small-scale vertically propagating internal gravity waves in the atmosphere or ocean, which are ultimately the object of this study. Consequently, in order to retain a simple two-dimensional model as a first numerical testbench, a modification of the SSW system was sought that would remove the unwanted gravity-wave shock formation. It can be shown that a modification of the pressure term corresponding to (6.1) with $\gamma = -1$ achieves this goal. Such a modification can easily be implemented in existing SSW numerical models, and, arguably, introduces only minimal changes in other features of the shallow-water model (Bühler 1997). The resulting model with $\gamma = -1$ is called the modified shallow-water model (MSW), and it was used in the simulations.†

The numerical scheme must have exceedingly low diffusion, including numerical diffusion, to capture the non-dissipative effects. This strongly suggests the ultimate use of specialized schemes, such as fast contour-dynamics schemes (Dritschel & Ambaum 1997), that obey the material invariance of PV by construction. However, up to now the application of such schemes has been confined to integrating balanced models, such as the quasi-geostrophic model, with the non-trivial extension of these schemes to the full shallow-water equations only now being actively pursued (Dritschel, personal communication). It therefore seemed prudent, in the first instance, to demonstrate the existence of the non-dissipative interaction effects using a SSW model, leaving the ultimately more promising pursuit of specialized schemes to further research.

8.1. Description of the numerical model and set-up

The numerical model used was that of Ford (1994), adapted to integrate the MSW equations in a beta-channel and to include a suitable wave generator. The model uses (u, v, h) as variables in the momentum and continuity equations, and is based on pseudospectral discretization in the zonal direction and on centred finite differences on a staggered grid in the meridional direction. Explicit leapfrog time stepping (with time step fixed at $2/3$ of the CFL condition) with Robert–Asselin filter constant equal to 0.03 is used (see Ford 1994 for details). The only systematic diffusion in the model interior is a small amount of hyperdiffusion, with damping rate νk^6 where k is the zonal wavenumber, that is applied in the zonal direction only, and which prevents numerical instability. The value of ν was fixed at $(4L/5N)^6 f_0$, where L is the zonal period length and N is the number of spectral coefficients, described below. Near the channel walls suitable Rayleigh damping is applied to all model fields, which allows removal of the gravity waves with negligible reflection over the span of two wavelengths (see below). Both hyperdiffusion and Rayleigh damping are treated implicitly in the time stepping.

The simplest possible channel set-up was chosen, with only a single wavetrain, as illustrated in figure 5. This set-up has the advantage that the small gravity-wave wavelength needs only to be resolved in the meridional direction, leaving only the much larger envelope scale to be resolved in the zonal direction. Therefore

† It is perhaps noteworthy that this MSW model is in fact the unique choice out of a slightly wider class of models than those in (6.1), namely all those models according to $c_0^2 \nabla h \rightarrow c_0^2 \nabla F(h)$ with *arbitrary* functions $F(\cdot)$, if one requires (a) that the linearized form of the pressure term remain unchanged, and (b) that simple one-dimensional non-rotating gravity waves can propagate in it without change in shape.

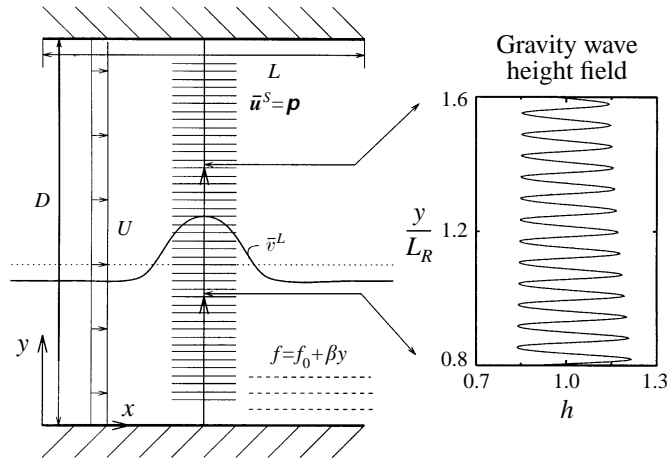


FIGURE 5. Left: set-up and displacement of a material contour in the early stages of the evolution. The contour is initially aligned zonally (dotted line), and subsequently it is dragged northward by the waves in the centre of the domain, and southward by a mass-conserving return flow at the sides (solid line). This is a typical displacement picture for large $L_R \geq L$, but not otherwise; see text. Right: insert illustrating the gravity-wave height field along the centreline of the middle region of the domain, in the case $D = 2.4L_R$. Near the boundaries, Rayleigh-damping sponge layers are imposed; see text.

resources can be focused on the meridional resolution, allowing these simulations to be performed on a workstation. All simulations reported below used highly anisotropic resolution with $N = 16$ spectral coefficients (i.e. 8 sines and 8 cosines) and 800 uniformly spaced grid intervals Δy across the channel, which allowed 20 grid intervals per gravity-wave wavelength. Over the last 40 grid intervals at each wall the Rayleigh damping rate is ramped up with a $\sin^2(\cdot)$ profile, with maximum damping rate fixed at $0.18 c_0/(\Delta y)$ at the wall.

A crucial requirement for the wave generator is that it must allow coherent wave forcing over hundreds of periods with minimal creation of artificial circulation. After some experimentation a body force derived from a time-dependent potential in the interior of the domain, near the southern wall, was chosen. The potential is proportional to a smooth envelope (in x and y) times $\sin(\hat{\omega}t) \cos(l y)$, where $\hat{\omega}^2 = f_0^2 + c_0^2 l^2$. This choice of potential force has the advantage that both its Eulerian and its leading-order Lagrangian average are zero. It generates gravity waves going both southward and northward, which turned out to be better conditioned numerically than generation of northward waves only. The southward-going waves are immediately absorbed at the nearby southern sponge layer. The wave generator is centred 80 grid intervals away from the southern wall, with meridional envelope given by a $\cos^2(\cdot)$ profile dropping from one to zero over 30 grid intervals, and zonal envelope given by a Gaussian with lengthscale $0.3L/4$. It should be noted that spurious local mass sources or sinks in a rotating fluid can lead to significant spin-up of corresponding spurious balanced motions due to the creation of PV anomalies, and it turned out to be crucial to discretize the y -derivatives in the continuity equation in flux form in order to avoid a slow loss of mass under the wave generator.

Owing to the anisotropic resolution the Eulerian average $\overline{(\cdot \cdot \cdot)}$ is implemented as a y -average over 60 grid intervals (i.e. 3 wavelengths). The diagnostics given below focus on the middle third of the channel, where the far-field theory of the previous

	L/L_R	D/L_R	$\beta D/f_0$	U/c_0	lL_R	a	$ \mathbf{p} /c_0 \approx \frac{1}{2} a^2$	Key feature
Case A	2.0	2.4	0.2	0.0	100	~ 0.17	~ 0.014	Irreversibility
Case B	2.0	2.4	0.2	0.0066	100	~ 0.17	~ 0.014	Resonance
Case C	20.0	24.0	0.2	0.0	10	~ 0.13	~ 0.008	Scale dependence

TABLE 2. Parameters for numerical simulations. Wave and pseudomomentum magnitudes correspond to the centre region of the channel

sections should be most applicable, and where the zonal components of $\bar{\mathbf{u}}^L$ and \mathbf{p} are both negligible.

8.2. Numerical simulations

Three different cases are investigated to demonstrate the irreversibility, the possible resonance, and the scale dependence of the mean-flow response. The parameters are summarized in table 2. The gravity waves have high frequencies in all three cases, which allows $f_0/\hat{\omega}$ to be neglected throughout. In the first two cases A and B the zonal wavetrain envelope scale $0.3L/4$ is much smaller than L_R , which allows the theoretical results obtained assuming $\epsilon \ll 1$ to be checked, and in case C the wavetrain envelope scale is larger than L_R , which allows the extensions of that theory to be checked.

Case A in figure 6 demonstrates irreversible wave-induced mean-flow changes that are left behind once the waves have been switched on and off. Case B differs from case A in that the waves are not switched off, and that a background flow $U > 0$ has been added that fulfils the resonance condition for the gravest channel mode (i.e. $n^* = 1$ in (4.4)). This leads to resonant growth of the PV deformations as demonstrated in figure 7. Finally, in case C all spatial scales have been multiplied by 10, and the drastically changed mean-flow response is shown in figure 8.

The mean-flow response in all cases can be understood qualitatively and quantitatively by considering the balanced mean-flow inversion operator (7.1). In cases A and B, the terms involving $1/L_R$ can be neglected, and \bar{v}^L follows $\rho_{(y)}$ closely until the PV anomaly $q - q_0$ becomes significant, either through resonance or because the waves are switched off again. In case C the $1/L_R$ terms are important, and (7.1) then shows that the mean flow reacts as if E were a mean-flow PV signal, with sign depending on the sign of $-A$. For high-frequency gravity waves in the MSW model (6.6) shows that $A = -1$, and hence the mean flow reacts as if E corresponded to positive mean-flow PV. This explains what is seen in figure 8, keeping in mind that E and the pseudomomentum magnitude have the same distribution, and that positive mean-flow vorticity corresponds to $\partial\bar{v}^L/\partial x > 0$ in the centre region.

This good agreement between theory and numerical simulation extends to a good estimate for \bar{h} from the far-field approximation (6.9) together with (7.1) and $A = -1$. In cases A and B, this predicts a level rise $c_0^2 \bar{h} \approx +E$, whereas in case C this predicts a much smaller level change that approaches zero as the $1/L_R$ terms become more and more dominant. Both predictions are well corroborated in the centre region of the numerical simulations.

9. GLM theory applied to the three-dimensional Boussinesq model

How does the foregoing generalize to the stratified systems that are of most interest in connection with the real atmosphere or oceans? It will turn out that, in contrast to the shallow-water model, only the pseudomomentum \mathbf{p}_2 enters the mean-flow

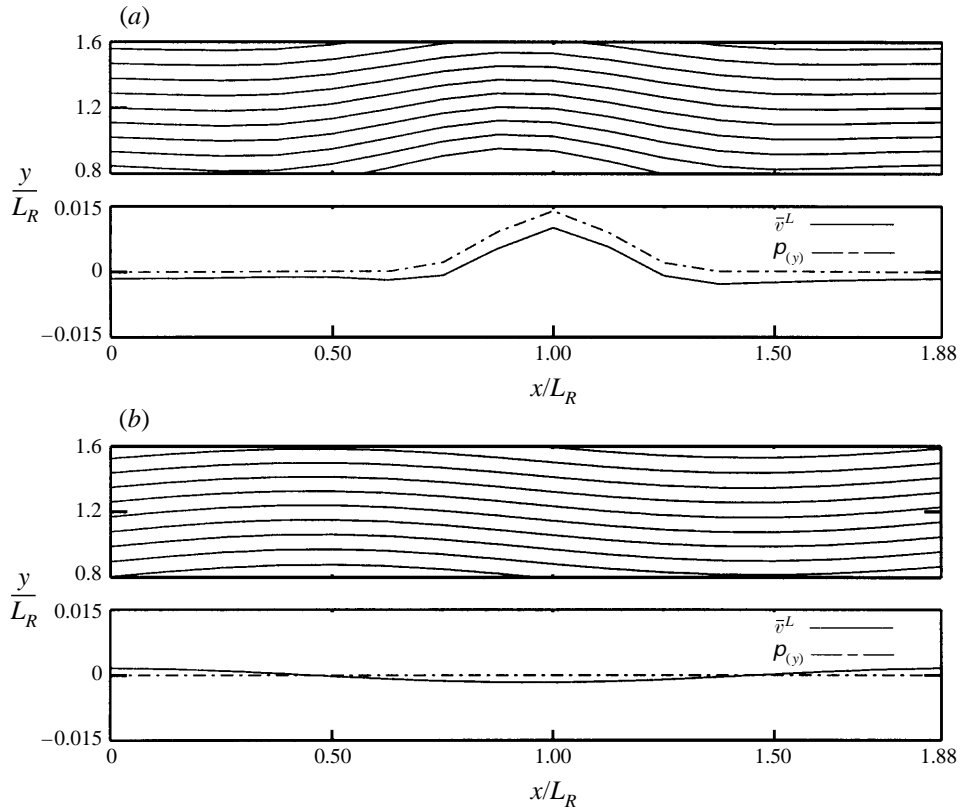


FIGURE 6. Case A. Two snapshots of averaged PV, \bar{v}^L , and $\rho_{(y)}$ at different times (a) $T = 25/f_0$, (b) $T = 100/f_0$. The upper panels show PV contours that originally filled the displayed middle section of the channel. The gravity waves are switched off at $T = 25/f_0$, and the deformed PV contours subsequently move to the left as a Rossby wave, demonstrating an irreversible mean-flow change. The lower panels show meridional pseudomomentum $\rho_{(y)}$ (broken line) and \bar{v}^L (solid line) plotted along the channel at $y = D/2$. Initially, \bar{v}^L follows $\rho_{(y)}$ closely, and after the waves have been switched off, \bar{v}^L is purely due to the mean-flow Rossby wave.

equations, i.e. E does not enter. Furthermore, \mathbf{p}_2 enters solely in the form of a forcing term $\nabla \times \mathbf{p}_2$. This is a remarkable simplification in comparison with the shallow-water model: it comes essentially from the simplifications inherent in the Boussinesq approximation.

Furthermore, in the simplest possible set of equations describing the balanced part of the $O(a^2)$ mean-flow response, only the vertical component of $\nabla \times \mathbf{p}_2$ enters. In this section we demonstrate these points by first deriving Boussinesq counterparts of the fully nonlinear PV equation (5.17) and the lemma (5.18), which exhibit the way in which the fully nonlinear pseudomomentum \mathbf{p} enters the problem. It turns out that the lemma is still true for arbitrary forces in the momentum equation, but only if the motion is adiabatic. That is, there must be no diabatic heating or cooling terms in order for the lemma to hold. Thereafter the entire $O(a^2)$ mean-flow response to slowly varying gravity waves is calculated, extending results first obtained in the non-rotating case by Bretherton (1969) to the rotating case with variable f . Finally, the simplest possible set of equations describing only the balanced part of the $O(a^2)$ mean-flow response is derived, using the quasi-geostrophic approximation as a balance condition.

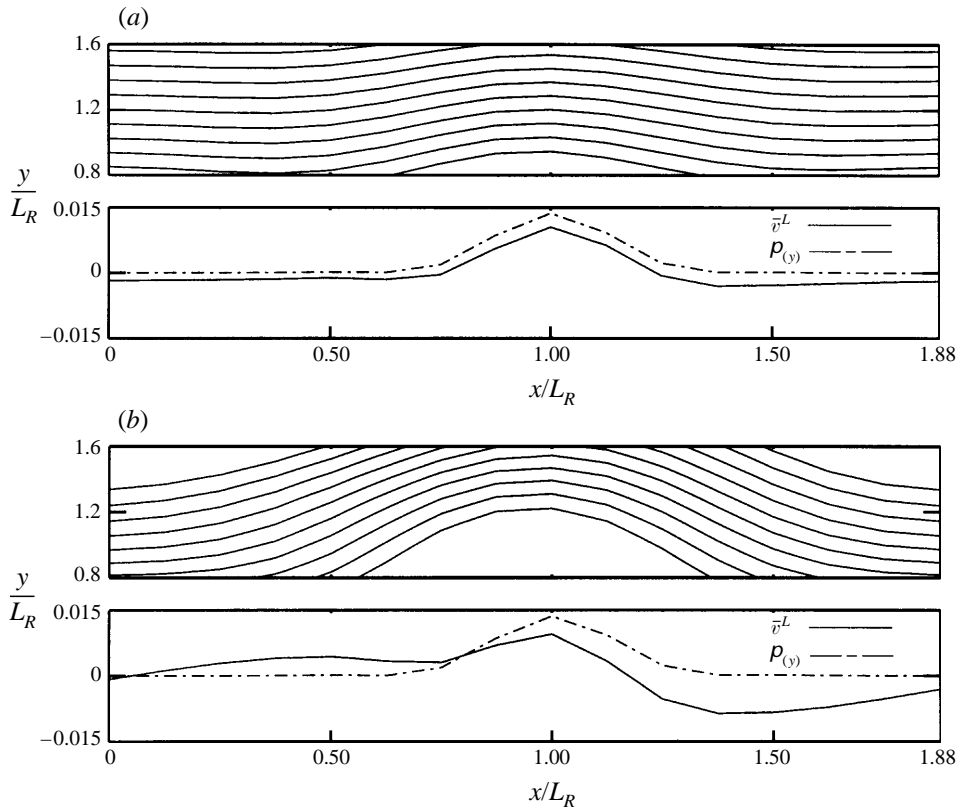


FIGURE 7. As for figure 6 but for Case B. Waves are continually radiated and a resonant background flow $U > 0$ has been added. PV contours deform resonantly, and \bar{v}^L departs from $p_{(y)}$ as the resonant Rossby-wave velocity field grows.

9.1. Nonlinear GLM results

The standard Boussinesq model is given by

$$\frac{D\mathbf{u}}{Dt} + \mathbf{f} \times \mathbf{u} + \nabla P = \sigma \hat{\mathbf{z}}, \quad (9.1)$$

$$\frac{D\sigma}{Dt} + N^2 w = 0, \quad (9.2)$$

together with the constraint $\nabla \cdot \mathbf{u} = 0$. The dependent variables are the three-dimensional velocity $\mathbf{u} = (u, v, w)$, the buoyancy acceleration σ , and P , the pressure deviation from hydrostatic pressure divided by the constant reference density. The Coriolis vector \mathbf{f} is either constant, or a non-divergent slowly varying vector field such that its Lagrangian disturbance part can be neglected, as was the case in the shallow-water β -plane. The buoyancy frequency N is taken to be constant, and the buoyancy acceleration σ in the vertical momentum equation expresses the gravitational restoring mechanism that opposes vertical displacements of the materially conserved stratification surfaces $\sigma + N^2 z$, which usually correspond to isentropes in the atmosphere and isopycnals in the ocean. The Boussinesq PV is a special case of

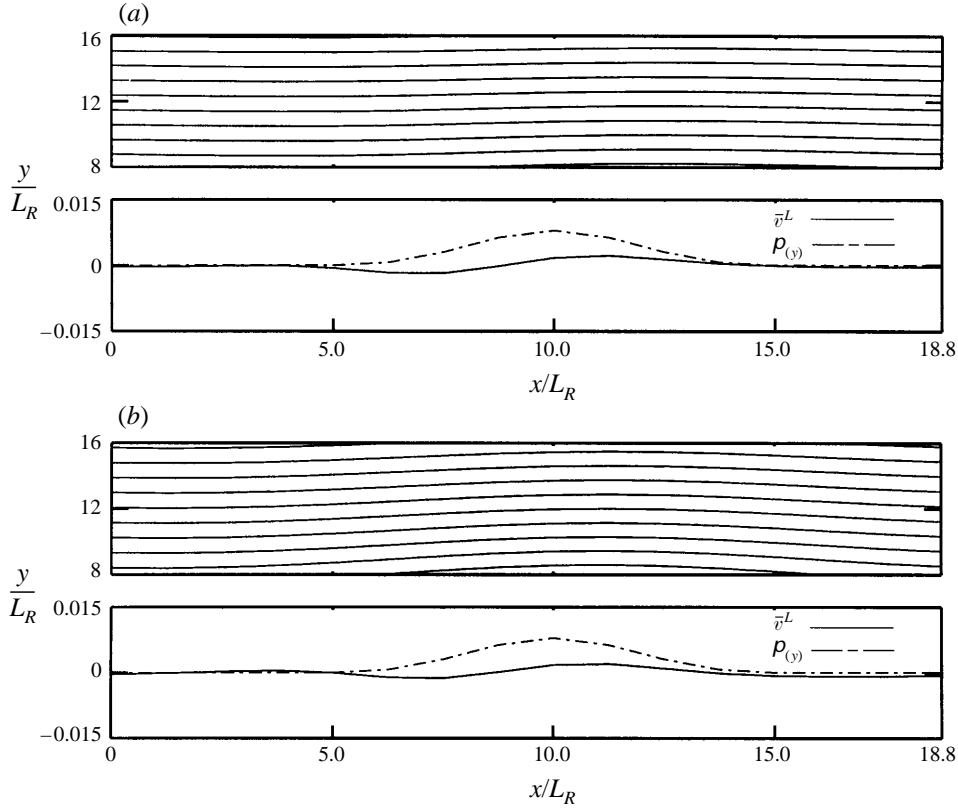


FIGURE 8. Case C. Spatial scales are enlarged by factor of 10 compared to A and B, leading to corresponding longer time integration as well: (a) $T = 250/f_0$, (b) $T = 1000/f_0$. Waves are continually radiated and background flow $U = 0$. See text for details on the changed mean-flow response.

(1.1) with $\theta = \sigma + N^2 z$ (up to a constant factor) and $\rho = 1$, i.e.

$$Q \equiv (\nabla \times \mathbf{u} + \mathbf{f}) \cdot \nabla (\sigma + N^2 z) \quad \Rightarrow \quad \frac{DQ}{Dt} = 0. \quad (9.3)$$

The GLM equations are derived by performing the same operations on (9.1) that were performed on the shallow-water momentum equations, which there lead to (5.15). This gives, in parallel with (3.8) of AM78a,

$$\overline{D}^L (\bar{u}_i^L - \mathbf{p}_i) + \bar{u}_{k,i}^L (\bar{u}_k^L - \mathbf{p}_k) + [\mathbf{f} \times \bar{\mathbf{u}}^L]_i + \bar{P}_i^L = \overline{(\dots)}_i + \bar{\sigma}^L \delta_{i3} + \bar{\sigma}^L \zeta_i, \quad (9.4)$$

where $\overline{(\dots)}_i$ is a complicated gradient term that will not affect the vorticity equation to be derived in the next step, ζ is the vertical disturbance-associated particle displacement such that

$$\overline{D}^L \zeta = w^l, \quad (9.5)$$

and the pseudomomentum \mathbf{p} is defined in its standard form $\mathbf{p}_i \equiv -\overline{(u_j^l + [\mathbf{f} \times \boldsymbol{\xi}]_j) \zeta_{j,i}}$. Equation (9.4) holds without approximation, except for the neglect of $(\mathbf{f}^l \times \mathbf{u}^l)$ in the case of varying \mathbf{f} .

The direct Lagrangian mean of (9.2) yields the pair

$$\overline{D}^L \overline{\sigma}^L + N^2 \overline{w}^L = 0 \tag{9.6}$$

and

$$\overline{D}^L \sigma^l + N^2 \overline{D}^L \zeta = 0, \tag{9.7}$$

where the disturbance equation follows directly from $\sigma^\xi = \overline{\sigma}^L + \sigma^l$, (9.5), and (5.9). The second equation can be integrated along mean trajectories, and yields (if there was no disturbance initially) $\sigma^l + N^2 \zeta = 0$. Therefore the last term in (9.4) can be written as a perfect gradient, i.e.

$$\overline{\sigma^l \zeta_i} = -N^2 \overline{(\zeta^2/2)_i}. \tag{9.8}$$

The curl of (9.4) then gives the GLM vorticity equation (cf. (5.15))

$$\begin{aligned} \overline{D}^L [\nabla \times (\overline{\mathbf{u}}^L - \boldsymbol{\rho}) + \mathbf{f}] + [\nabla \times (\overline{\mathbf{u}}^L - \boldsymbol{\rho}) + \mathbf{f}] \nabla \cdot \overline{\mathbf{u}}^L \\ - ([\nabla \times (\overline{\mathbf{u}}^L - \boldsymbol{\rho}) + \mathbf{f}] \cdot \nabla) \overline{\mathbf{u}}^L = \nabla \overline{\sigma}^L \times \hat{\mathbf{z}}. \end{aligned} \tag{9.9}$$

This equation expresses that the mean vector field [...] is advected by the mean velocity field $\overline{\mathbf{u}}^L$ in exactly the same way as is $\nabla \times \mathbf{u}$ by the actual velocity field \mathbf{u} , i.e. [...] is advected and stretched/twisted by $\overline{\mathbf{u}}^L$ (first and third terms on the left-hand side) and diluted/concentrated by $\nabla \cdot \overline{\mathbf{u}}^L$ (second term on the left-hand side). The baroclinic force-curl on the right-hand side represents the gravity-wave restoring mechanism; it too enters in exactly the same way as does $\nabla \sigma \times \hat{\mathbf{z}}$ in the actual vorticity equation.

Defining the GLM density $\tilde{\rho}$ in the usual way through

$$\overline{D}^L \tilde{\rho} + \tilde{\rho} \nabla \cdot \overline{\mathbf{u}}^L = 0, \tag{9.10}$$

and noting that (9.6) implies that

$$\overline{D}^L (\overline{\sigma}^L + N^2 z) = 0 \tag{9.11}$$

and

$$\overline{D}^L (\overline{\sigma}_{,i}^L + N^2 \delta_{i3}) + \overline{u}_{k,i}^L \overline{\sigma}_{,k}^L + N^2 \overline{w}_{,i}^L = 0, \tag{9.12}$$

we can show, using (9.6), (9.9), and (9.12), that

$$\tilde{Q} \equiv \frac{[\nabla \times (\overline{\mathbf{u}}^L - \boldsymbol{\rho}) + \mathbf{f}] \cdot \nabla (\overline{\sigma}^L + N^2 z)}{\tilde{\rho}} \Rightarrow \overline{D}^L \tilde{Q} = 0, \tag{9.13}$$

which is the Boussinesq analogue of the shallow-water equation (5.17). The Lagrangian mean of (9.3) gives $\overline{D}^L \overline{Q}^L = 0$ by (5.9), and hence, as before, if $\tilde{Q} = \overline{Q}^L$ initially then it holds at all times.

This derivation of \tilde{Q} can easily be extended to the fully compressible three-dimensional Euler equations, without the restriction to constant N^2 . In that case ρ can vary and the usual definition of PV is given by the Rossby–Ertel formula (1.1). The potential temperature θ is materially conserved, i.e. $D\theta/Dt = 0$. Starting from (3.8) in AM78a, and noting that θ is a monotonically increasing function of entropy, the corresponding \tilde{Q} is found to be (9.13) with the substitution $\overline{\theta}^L$ for $\overline{\sigma}^L + N^2 z$.

Furthermore, it can be shown that, subject only to suitable initialization with no initial disturbance, $\tilde{Q} = \overline{Q}^L$ holds even if arbitrary body forces are added to the momentum equations, but, interestingly, not if diabatic heating or cooling is added

to the buoyancy equation (9.2). This applies to both Boussinesq and Euler equations, and the proof is given here for the more general Euler case. Consider two volumes V and V^ξ , where V^ξ is the image of V under the lifting map $\mathbf{x} \rightarrow \mathbf{x} + \boldsymbol{\xi}$, and let a scalar S be defined as

$$S \equiv \int \int \int_{V^\xi} Q \rho \, dV = \int \int \int_V Q^\xi \tilde{\rho} \, dV = \int \int \int_V (\nabla \times \mathbf{u} + \mathbf{f})^\xi \cdot (\nabla \theta)^\xi \frac{\tilde{\rho}}{\rho^\xi} \, dV, \quad (9.14)$$

where (5.11) has been used. Using (A4) and (A17) of AM78a to relate $(\nabla \theta)^\xi$ to $\nabla(\theta^\xi)$ and to relate the vorticity vector at $\mathbf{x} + \boldsymbol{\xi}$ to $\nabla \times (\bar{\mathbf{u}}^L - \boldsymbol{\rho})$ then gives, using (5.11) again,

$$S = \int \int \int_V (\nabla \times (\bar{\mathbf{u}}^L - \boldsymbol{\rho}) + \mathbf{f} + \boldsymbol{\Delta}') \cdot \nabla(\theta^\xi) \, dV \quad \text{where} \quad \overline{\boldsymbol{\Delta}'} = 0. \quad (9.15)$$

The zero-mean disturbance vector $\boldsymbol{\Delta}'$, whose details are irrelevant here, is defined to be the fluctuating part of the expression on the left-hand side of AM78a's (A 17) before averaging. This represents zero-mean fluctuations of the absolute vorticity vector that are induced by the fluctuating material displacements $\boldsymbol{\xi}$. Taking the average of (9.15) then gives, after comparison with (9.13) and noting that $\bar{\theta}^L = \bar{\sigma}^L + N^2 z$ there,

$$\overline{S} = \int \int \int_V [\bar{Q} \bar{\rho} + \overline{(\boldsymbol{\Delta}' \cdot \nabla \theta^l)}] \, dV. \quad (9.16)$$

On the other hand, averaging the second expression in (9.14) gives

$$\overline{S} = \int \int \int_V \bar{Q}^L \tilde{\rho} \, dV. \quad (9.17)$$

Therefore, if it is now assumed that $\theta^l = 0$, then (9.16) and (9.17) and the arbitrariness of V imply that $\bar{Q} = \bar{Q}^L$, i.e. that

$$\boxed{\bar{Q}^L = \bar{Q} = \frac{(\nabla \times (\bar{\mathbf{u}}^L - \boldsymbol{\rho}) + \mathbf{f}) \cdot \nabla \bar{\theta}^L}{\tilde{\rho}}}. \quad (9.18)$$

The condition $\theta^l = 0$ will, in general, only be fulfilled if the flow is initialized without disturbance, as has been assumed throughout, and if there is no diabatic heating or cooling, i.e. if $D\theta/Dt = 0$ holds. However, arbitrary forces can be added in the momentum equation without violating (9.18). Hence, in the absence of diabatic heating or cooling a lemma analogous to the lemma for the shallow-water system, (5.18), holds in the three-dimensional stratified case.

9.2. Small-amplitude GLM results

The $O(a^2)$ mean-flow response to small-amplitude, slowly modulated inertia-gravity waves is now derived. The Coriolis vector is taken to be $\mathbf{f} = \hat{\mathbf{z}}(f_0 + \beta y)$ with $\beta L \ll f_0$, where L is the horizontal envelope scale of the waves. A weak $O(1)$ background zonal flow $\mathbf{U} = \hat{\mathbf{x}}U(y, z)$ may be present, with $U/L \ll f_0$, $U_z \ll N$, and $U_{,yy} \sim U/L^2 \sim \beta$. The weakness of \mathbf{U} allows the background part of $\bar{\sigma}^L$ to be neglected.

The near-plane $O(a)$ inertia-gravity waves have wavenumber vector $\mathbf{k} = (k, l, m)$ and are slowly modulated with horizontal and vertical envelope scales L and H , respectively. This implies that the wavenumber vector magnitude $\kappa = (k^2 + l^2 + m^2)^{1/2}$

satisfies $\kappa L \gg 1$ and $\kappa H \gg 1$. The dispersion relation is

$$\hat{\omega}^2 = f_0^2 \frac{m^2}{\kappa^2} + N^2 \frac{k^2 + l^2}{\kappa^2}, \quad (9.19)$$

which implies that $|\hat{\omega}| > f_0 \gg \beta L$. It turns out that there is no leading-order Stokes drift, but the leading-order pseudomomentum is still given by the generic formula

$$\mathbf{p}_2 = \frac{\mathbf{k}}{\hat{\omega}} E \quad \text{and} \quad |\nabla \times \mathbf{p}_2| \sim \frac{1}{\min(L, H)} \frac{\kappa}{\hat{\omega}} E, \quad (9.20)$$

where $E = \frac{1}{2}(\overline{|\mathbf{u}'_1|^2} + N^{-2}\overline{\sigma_1'^2})$ is the average intrinsic wave energy per unit mass of the inertia-gravity waves.

The full $O(a^2)$ mean-flow response consists of the five fields $\tilde{\rho}_2$, $\bar{\sigma}_2^L$, and $\bar{\mathbf{u}}_2^L$. However, the constraint $\nabla \cdot \mathbf{u} = 0$ implies that (cf. (9.4) in AM78a)

$$\nabla \cdot \bar{\mathbf{u}}^L = \frac{1}{2} D_t (\overline{\xi_i' \xi_j'})_{,ij} + O(a^3) = D_t O\left(\frac{E}{\hat{\omega}^2 \min(L^2, H^2)}\right), \quad (9.21)$$

where $D_t = \partial/\partial t + \mathbf{U} \cdot \nabla$. This shows that $\nabla \cdot \bar{\mathbf{u}}_2^L$ is inherently linked to gravity-wave transience. Furthermore, comparing the size of the divergence term in the vorticity equation (9.9) with the size of the first term in that equation gives, using (9.20),

$$\frac{f_0 \nabla \cdot \bar{\mathbf{u}}_2^L}{D_t \nabla \times \mathbf{p}_2} \sim \frac{f_0}{\hat{\omega}} \frac{1}{\min(\kappa L, \kappa H)} \ll 1. \quad (9.22)$$

Hence, unlike in the shallow-water case, it is possible to neglect $\nabla \cdot \bar{\mathbf{u}}_2^L$ at all times on order-of-magnitude grounds, even when the waves are transient. This depends crucially on the slow-modulation assumption in all directions, and would fail, for instance, in the case of surface gravity waves as discussed in McIntyre (1988). The smallness of $\nabla \cdot \bar{\mathbf{u}}_2^L$ implies that $\tilde{\rho}_2$ can be neglected at all times as well, and hence the only remaining fields to be determined are $\bar{\sigma}_2^L$ and $\bar{\mathbf{u}}_2^L$, subject to $\nabla \cdot \bar{\mathbf{u}}_2^L = 0$.

The $O(a^2)$ parts of (9.6) and (9.9) provide the necessary equations as

$$D_t \bar{\sigma}_2^L + N^2 \bar{w}_2^L = 0 \quad (9.23)$$

and

$$D_t [\nabla \times (\bar{\mathbf{u}}_2^L - \mathbf{p}_2)] + (\bar{\mathbf{u}}_2^L \cdot \nabla) (\mathbf{f} + \nabla \times \mathbf{U}) - ([\nabla \times (\bar{\mathbf{u}}_2^L - \mathbf{p}_2)] \cdot \nabla) \mathbf{U} - ((\mathbf{f} + \nabla \times \mathbf{U}) \cdot \nabla) \bar{\mathbf{u}}_2^L = \nabla \bar{\sigma}_2^L \times \hat{\mathbf{z}}. \quad (9.24)$$

For any given $\nabla \times \mathbf{p}_2$ these two equations together with $\nabla \cdot \bar{\mathbf{u}}_2^L = 0$ determine the full mean-flow response, which includes both balanced parts such as mean-flow Rossby waves and unbalanced parts such as mean-flow gravity waves.

The simplest diagnostic equations for the balanced part of the mean-flow response can be derived using the usual quasi-geostrophic balance conditions. These follow from (9.23) and (9.24) by assuming sufficiently slow evolution such that the time derivatives can be neglected at leading order, and by assuming sufficiently strong background rotation such that the undifferentiated f_0 sets the dominant scale in (9.24). This leads to $\bar{w}_2^L = 0$ and $f_0 \partial \bar{\mathbf{u}}_2^L / \partial z = \nabla \bar{\sigma}_2^L \times \hat{\mathbf{z}}$ as balance conditions. These conditions can be satisfied by introducing the quasi-geostrophic stream function Ψ^L such that

$$\bar{u}_2^L = -\Psi_y^L, \quad \bar{v}_2^L = +\Psi_x^L, \quad \bar{w}_2^L = 0, \quad \bar{\sigma}_2^L = f_0 \Psi_z^L. \quad (9.25)$$

Substituting (9.25) in the $O(a^2)$ part of (9.13), which is

$$\tilde{Q} = N^2 (f_0 + \beta y - U_y) + N^2 [\nabla \times (\bar{\mathbf{u}}_2^L - \mathbf{p}_2)] \cdot \hat{\mathbf{z}} + (\mathbf{f} + \nabla \times \mathbf{U}) \cdot \nabla \bar{\sigma}_2^L + O(a^3), \quad (9.26)$$

then gives the diagnostic equations.

The prognostic equation is obtained by using in (9.26) in (9.13), keeping only the dominant f_0 factor in the term involving $\bar{\sigma}_2^L$. This yields

$$\boxed{D_t \left[\Psi_{xx}^L + \Psi_{yy}^L + \frac{f_0^2}{N^2} \Psi_{zz}^L \right] + \Psi_x^L (\beta - U_{yy}) = D_t [\nabla \times \mathbf{p}_2] \cdot \hat{\mathbf{z}}}, \quad (9.27)$$

or, equivalently to $O(a^2)$,

$$\boxed{(D_t + \bar{\mathbf{u}}_2^L \cdot \nabla) \tilde{Q} = 0} \quad (9.28)$$

and

$$\boxed{\Psi_{xx}^L + \Psi_{yy}^L + \frac{f_0^2}{N^2} \Psi_{zz}^L = \frac{\tilde{Q}}{N^2} - (f_0 + \beta y - U_y) + [\nabla \times \mathbf{p}_2] \cdot \hat{\mathbf{z}}}, \quad (9.29)$$

where the last two equations makes the prognostic and diagnostic parts of the balanced evolution explicit.

In the simplest case $\beta = 0$ and $U = 0$ there is no background gradient of \tilde{Q} and hence the solution of (9.28) is simply $\tilde{Q} = f_0 N^2$. The diagnostic equations (9.29) and (9.25) then demonstrate the purely transient, layer-wise two-dimensional $O(a^2)$ mean motions due to gravity waves that were first pointed out by Bretherton (1969) in the special case $f_0 = 0$. If $\beta \neq 0$, irreversible forcing of $O(a^2)$ Rossby waves by the $O(a)$ gravity waves takes place. This is fundamentally similar to the case of the shallow-water system. The robustness with which $\nabla \times \mathbf{p}_2$ enters the balanced mean-flow problem in both cases is intriguing.

10. Concluding remarks

Although most of the foregoing analysis is for the shallow-water system, it has also become clear, from §9, that certain broad conclusions will carry over to more realistic stratified systems provided that we use the pseudomomentum, and not the Stokes drift, as the principal field describing the non-dissipative effects of the waves on the mean motion. This came as a surprise in view of the heuristic idea that advection of PV contours by the Stokes drift ought to be at least one of the significant effects. But, in the manner typical of wave-mean problems, the Stokes drift is not the only significant effect, and it can be cancelled by other effects of the same order. Another surprise was that the cross-stream mean force $\mathbf{p}_2 \cdot \hat{\mathbf{x}} \partial U / \partial y$ appearing in the second term of the GLM momentum equation (5.15) has no visible role, even though its magnitude is not always negligible. Such a mean force might at first be thought to be significant for exciting the Rossby-wave response in the zonally asymmetric mean dynamics. The explanation is, again, that there are other effects of the same order and that only the net effect, allowing for mutual cancellations, is relevant. Such cancellations are indeed part of why, in the end, the PV-centred viewpoint turns out to be much simpler than any momentum-based viewpoint.

The last finding is itself non-trivial, because generally speaking the usual concepts of balance and PV inversion need to be modified to an extent that is non-trivial, in wave-mean problems of the present type. This is in marked contrast to dissipative wave-mean problems of the kind discussed in McIntyre & Norton (1990), who

assumed balance in the ordinary sense to be a sufficient approximation. The example studied in §§6 and 8 illustrates the point, which emerges clearly in one of the parameter regimes analysed. Radiation stresses modify, at leading order, the geostrophic balance that would otherwise be expected at low Rossby number; and this changes the velocity profile *qualitatively* (cf. figure 7 and figure 8), providing, also, a first example in which the advection of PV contours is qualitatively different from that expected from a naive consideration of Stokes drifts alone.

More generally, non-dissipating gravity waves induce certain modifications in the diagnostic step of the balanced evolution, cf. (1.3) and (1.4). Recognizing these modifications complements and clarifies our picture of the coupled, side-by-side evolution of balanced and unbalanced parts of the flow. Furthermore, recognizing the possible cumulative importance of these non-dissipative modifications corrects the standard assumption that the only important effects are dissipative.

As regards practical implications for atmosphere or ocean dynamics, such as the design of gravity-wave drag parametrizations for atmospheric circulation and chemistry models, this work suggests that the main places to look for strong, cumulative, non-dissipative interaction effects are situations that allow, and are close to, Rossby-wave resonance. This is the other important conclusion that we expect to carry over to stratified systems. Conversely, in the absence of Rossby-wave resonance these non-dissipative interaction effects are likely to be quite weak. The relevance of Rossby-wave resonance for important phenomena such as, e.g., stratospheric summer warmings is still very much a topic of current research and an area of uncertainty. This means that at present the practical relevance of non-dissipative wave–mean interaction effects remains an open question.

O. B. thanks the Gottlieb Daimler and Karl Benz foundation in Germany and the Natural Environment Research Council (NERC) for research studentships, and NERC for further post-doctoral funding under grant GR9/01907. M. E. M. thanks the Engineering and Physical Sciences Research Council for generous support in the form of a Senior Research Fellowship.

The Centre for Atmospheric Science is a joint initiative of the Department of Chemistry and the Department of Applied Mathematics and Theoretical Physics.

Appendix. Details of the evolution of \bar{h}_2 and the accuracy of far-field expression (6.9)

A.1. Boundary condition for \bar{h}_2 and the far-field approximation

At an impermeable (although possibly undulating) wall the GLM velocity perpendicular to the mean position of the wall vanishes (cf. §4.2 in AM78*a*). To $O(a^2)$ this means that $\bar{v}_2^L = 0$ at $y = 0$ and $y = D$, and if this condition is used in the y -component of the $O(a^2)$ part of the GLM momentum equation (5.15) (with modified pressure term according to (6.11)), then the boundary condition for \bar{h}_2 results. Noting that in general $\overline{u_j^\xi u_j^\xi} = \overline{u_j^L u_j^L} + \overline{u_j^l u_j^l}$, that $\overline{u_j^\xi (f_0 \hat{z} \times \xi)_j} = \overline{u_j^l (f_0 \hat{z} \times \xi)_j}$, and that $\mathbf{u}^l \approx \mathbf{u}'_1$ by (5.29) simplifies the momentum equation. The $O(a)$ inertia–gravity-wave fields derived previously have to be used to evaluate the correlations between \mathbf{u}'_1 and ξ' . This is most easily done by choosing the local wavenumber vector to be $\mathbf{k} = (k, 0)$, without loss of generality, which yields (cf. (3.12) and (3.13))

$$\overline{u_j^l u_j^l} + \overline{u_j^l (f_0 \hat{z} \times \xi)_j} \approx \overline{u_1'^2} - \overline{v_1'^2} = \overline{u_1'^2} \left(1 - \frac{f_0^2}{\hat{\omega}^2} \right) = E \left(1 - \frac{f_0^2}{\hat{\omega}^2} \right) \quad (\text{A } 1)$$

for the remaining terms on the right-hand side of (5.15). The last expression holds regardless of any specific choice of \mathbf{k} . Taylor-expanding the pressure term on the left-hand side of (5.15), subtracting a Stokes correction \bar{h}_2^S corresponding to (5.35) and (3.15), and using $\bar{D}^L \approx \partial/\partial t$ finally leads to

$$f_0 \bar{u}_2^L + c_0^2 \bar{h}_{2,y} = \rho_{(y),t} + \left(1 - \frac{f_0^2}{\hat{\omega}^2}\right) \frac{1-\gamma}{2} E_{,y} \quad \text{at } y = 0 \text{ and } y = D. \quad (\text{A } 2)$$

Suffixes denote differentiation, and $\rho_{(y)} = El/\hat{\omega}$ denotes the y -component of the pseudomomentum vector. This boundary condition uses the same approximations as the simplified divergence equation (6.5)

$$\left(\frac{\partial^2}{\partial t^2} - c_0^2 \nabla^2\right) \bar{h}_2 + f_0 \nabla \times \bar{\mathbf{u}}_2^L = \left(\frac{\partial^2}{\partial t^2} + c_0^2 A \nabla^2\right) \frac{E}{c_0^2}, \quad (\text{6.5})$$

i.e. it neglects U and β . Given the time-dependent E and $\rho_{(y)}$, the spin-up of $\nabla \times \bar{\mathbf{u}}_2^L$ and \bar{h}_2 is then described by (A 2), (6.5), and the vorticity equation in the form (6.7).

For steady gravity waves \bar{h}_2 is given by the far-field expression (6.9) together with a harmonic remainder term, i.e.

$$c_0^2 \bar{h}_2 = f_0 \Psi^L - \Lambda E + R \quad \text{with} \quad \nabla^2 R = 0, \quad (\text{A } 3)$$

where Λ is defined in (6.6), and where Ψ^L is the stream function for $\bar{\mathbf{u}}_2^L$ introduced previously. Note that it was part of the definition of Ψ^L that it should have zero integral over the channel. The boundary conditions for R follow from (A 2) and (6.6) as

$$R_{,y} = \frac{f_0^2}{\hat{\omega}^2} E_{,y} \quad \text{at } y = 0 \text{ and } y = D, \quad (\text{A } 4)$$

which, remarkably, has no dependence on γ but depends crucially on f_0 . The harmonic remainder R can be decomposed into zonal spectral modes proportional to $\exp(iKx)$, with coefficients fixed by (A 4). For $K \neq 0$ the corresponding meridional mode structure is $\exp(\pm Ky)$, which leads to the exponential decay of the $K \neq 0$ modes away from the boundaries. For $K = 0$ the meridional mode structure is $a + by$, with two constants a and b . The constant b is proportional to the zonal average of (A 4). However, in the steady situation envisaged here E is constant along parallel straight rays originated at the wall forcing regions. This implies that

$$\int_0^L E(x, y)_{,y} dx = \frac{d}{dy} \int_0^L E(x, y) dx = 0 \quad (\text{A } 5)$$

for all y , and hence $b = 0$. The constant a is not determined by (A 4). However, the constant a can be determined by requiring, for instance, that the total mass in the channel be conserved, which means that the integral over the entire channel of \bar{h}_2 as given by (A 3) has to be zero. This will give a value for a that is proportional to the energy density of the waves times the ratio of the area covered by the wavetrains and the area of the channel. Consequently, if the wavetrains fill only a small part of the channel then a will be small.

In summary, the accuracy of the steady-state far-field approximation (6.9) is seen to be limited by two factors. First, there are deviations near the walls if the gravity waves are of low frequency and the wavetrains are tilting in the horizontal direction. These deviations are induced by (A 4). Second, if the wavetrains occupy a significant part of the area of the channel, then global mass conservation would make the

global constant a significant in (A 3). Conversely, sparse wavetrains far away from boundaries can be expected to satisfy (6.9) accurately.

A.2. Non-rotating special case and one-dimensional wavetrains

If f_0 is sufficiently weak such that $f_0\Psi^L$ can be neglected in (A 3), then it is possible to derive a typical structure of \bar{h}_2 that depends only on E . The simplest possible example has $f_0 = 0$ and only a single wavetrain emitted at the southern wall and propagating across the channel in a straight line. The condition (A 4) is then homogeneous and therefore $R = a$, where a is a constant determined by mass conservation. This means that

$$c_0^2 \bar{h}_2 = -\frac{\gamma - 1}{2} E + a \tag{A 6}$$

in this example. If the width of the smoothly varying wavetrain envelope is denoted by d , then it is clear that $a \sim d/L$ as $d/L \rightarrow 0$, which can be achieved without violating the JWKB requirement $\kappa d \gg 1$ by letting L grow whilst keeping d constant. Therefore, for a sufficiently large channel the height field approaches (A 6) with $a = 0$. Remarkably, for standard shallow water (i.e. $\gamma = 2$) this corresponds to a mean height decrease in the wavetrain, whereas for modified shallow water (i.e. $\gamma = -1$) this corresponds a mean height increase there. This structure of \bar{h}_2 remains typical as long as f_0 is weak. For instance, it has to good approximation been observed in those numerical simulations in §8 in which $L/L_R \ll 1$.

It is of some interest to know what the counterpart of (A 6) may be in the case of a truly one-dimensional wavetrain, in which gravity waves are forced along the entire channel wall and the wavetrain envelope is therefore effectively infinite. For instance, this would be the typical situation in the case of acoustic piston-type problems that involve wave propagation along tubes. This one-dimensional case differs in two important respects from the two-dimensional case. First, in the two-dimensional case the mean pressure field inside the wavetrain has to match up with the ambient background pressure far away from the wavetrain, whereas in the one-dimensional case the mean pressure may be different from the background pressure everywhere. Second, the influence of the wall boundaries in the two-dimensional case decays with increasing distance from the walls, and becomes small when this distance is sufficiently large compared to the envelope scale of the wavetrain. In the one-dimensional case the envelope scale is effectively infinite, and hence it is to be expected that the influence of the wall boundaries does not decay.

This can be illustrated by considering a simple one-dimensional time-dependent spin-up problem with $f_0 = 0$ and $\mathbf{k} = (0, l)$, which can be solved explicitly. The waves are generated at the southern boundary and propagate northward with speed c_0 . In this case (cf. (3.20))

$$E = E_0 F(c_0 t - y) \quad \text{and} \quad p_{(y)} = \frac{E_0}{c_0} F(c_0 t - y), \tag{A 7}$$

where E_0 is the positive value of wave energy after spin-up, and $F(\cdot)$ is a smooth switch-on function that varies from zero to unity as its argument varies from zero to $O(D)$ and then remains unity for larger values of its argument. The right-hand sides of (A 2) and (6.5) then become

$$\frac{\gamma + 1}{2} E_0 F'(c_0 t) \quad \text{and} \quad \frac{\gamma + 1}{2} E_0 F''(c_0 t - y) \tag{A 8}$$

respectively, where F', F'' denotes differentiation of F with respect to its argument.

Both equations together allow an easy determination of \bar{h}_2 for times small enough such that the wavetrain has not yet reached the northern boundary, where reflection might take place. The solution for these times is

$$c_0^2 \bar{h}_2 = -E_0 \frac{\gamma + 1}{4} \frac{\partial}{\partial y} (y F(c_0 t - y)), \quad (\text{A } 9)$$

which in particular implies a steady height change

$$c_0^2 \bar{h}_2 = -E_0 \frac{\gamma + 1}{4} \quad (\text{A } 10)$$

at positions y well inside the wavetrain such that $F \approx 1$ there. The height field is constant except at the wave front where F varies significantly. At the wave front there is a secularly growing change in \bar{h}_2 . In the special case $\gamma = -1$ there would be no change in \bar{h}_2 anywhere, in contrast with the two-dimensional result for $\gamma = -1$ following from (A 6), which is $\bar{h}_2 = E/c_0^2$. An independent check on (A 8) hence (A 10) comes from the standard expression $E_0(1 + \partial \ln c / \partial \ln \rho)$ for the longitudinal acoustic radiation stress (Brillouin 1925, 1936; McIntyre 1981), which translates here to $E_0(\gamma + 1)/2$.

The steady-state result (A 10) admits yet another independent check using Riemann's theory of characteristics (e.g. Whitham 1974). This theory, when applied to simple waves generated at $y = 0$ and propagating into a semi-infinite region $y > 0$ that was previously at rest, states that the nonlinear algebraic relation

$$\frac{\gamma - 1}{2} v + c_0 = c_0 h^{(\gamma-1)/2} \quad (\text{A } 11)$$

holds everywhere. Taking a Eulerian average at steady state, Taylor-expanding, collecting terms at $O(a^2)$, and using (5.35) gives the relation

$$\bar{v}_2 = c_0 \bar{h}_2 + \frac{\gamma - 3}{4} \frac{E}{c_0}. \quad (\text{A } 12)$$

The Lagrangian-mean velocity $\bar{v}_2^L = 0$ at $y = 0$ and in fact everywhere except at the wave front. Therefore $\bar{v}_2 = -\bar{v}_2^S = -E/c_0$, and hence (A 10) is recovered by this independent route.

This shows again the importance of the boundary condition at $y = 0$. The boundary condition at $y = D$, i.e. at the other channel side, is equally important: non-reflecting conditions to $O(a)$ and $O(a^2)$ mean that (A 9) is valid at all times, but in this case (A 10) implies that the channel must change its total mass content (unless $\gamma = -1$), i.e. $\bar{v}_2^L \neq 0$ at $y = D$ when the wave front arrives. On the other hand, a non-reflecting boundary condition to $O(a)$ only can be combined with total mass conservation, but then there will be a back-reflected $O(a^2)$ wave in \bar{h}_2 that continually propagates back and forth across the channel. If a small amount of damping is imagined, then this $O(a^2)$ wave eventually dies out and establishes $\bar{h}_2 = 0$ throughout the channel, which is the only steady height configuration compatible with mass preservation.

Unlike the two-dimensional cases studied previously, the one-dimensional case depends globally, i.e. at long range, on the exact boundary conditions and the exact initial conditions of the flow. This highlights, for instance, the very special character of the problems with spatially-periodic disturbance velocity potential studied in Yih (1997), which rules out *ab initio* all $O(a^2)$ effects like that described by (A 10).

REFERENCES

- ANDREWS, D. G., HOLTON, J. R. & LEOVY, C. B. 1987 *Middle Atmosphere Dynamics*. Academic Press, 489 pp.
- ANDREWS, D. G. & MCINTYRE, M. E. 1978*a* An exact theory of nonlinear waves on a Lagrangian-mean flow. *J. Fluid Mech.* **89**, 609–646 (referred to herein as AM78*a*)
- ANDREWS, D. G. & MCINTYRE, M. E. 1978*b* On wave-action and its relatives. *J. Fluid Mech.* **89**, 647–664 (and Corrigendum **95**, 796) (referred to herein as AM78*b*)
- BRETHERTON, F. P. 1969 On the mean motion induced by internal gravity waves. *J. Fluid Mech.* **36**, 785–803.
- BRILLOUIN, L. 1925 On radiation stresses. *Ann. Phys.* **4**, 528–586 (in French).
- BRILLOUIN, L. 1936 On radiation pressures and stresses. *Rev. d'Acoust.* **5**, 99–111 (in French).
- BRILLOUIN, L. 1964 *Tensors in Mechanics and Elasticity*. Academic.
- BÜHLER, O. 1996 Waves and balanced mean flows in the atmosphere. PhD thesis, University of Cambridge, 183 pp.
- BÜHLER, O. 1997 A shallow-water model that prevents nonlinear steepening of gravity waves. *J. Atmos. Sci.* (submitted).
- DRITSCHEL, D. G. & AMBAUM, M. H. P. 1997 A contour-advective semi-Lagrangian numerical algorithm for simulating fine-scale conservative dynamical fields. *Q. J. R. Met. Soc.* **123**, 1097–1130.
- FORD, R. 1994 Gravity wave radiation from vortex trains in rotating shallow water. *J. Fluid Mech.* **281**, 81–118.
- HOLTON, J. R., HAYNES, P. H., MCINTYRE, M. E., DOUGLASS, A. R., ROOD, R. B. & PFISTER, L. 1995 Stratosphere–troposphere exchange. *Rev. Geophys.* **33**, 403–439.
- HOSKINS, B. J., MCINTYRE, M. E. & ROBERTSON, A. W. 1985 On the use and significance of isentropic potential-vorticity maps. *Q. J. R. Met. Soc.* **111**, 877–946. See also **113**, 402–404.
- MCINTYRE, M. E. 1981 On the “wave momentum” myth. *J. Fluid Mech.* **106**, 331–347.
- MCINTYRE, M. E. 1988 A note on the divergence effect and the Lagrangian-mean surface elevation in water waves. *J. Fluid Mech.* **189**, 235–242.
- MCINTYRE, M. E. 1993 Isentropic distributions of potential vorticity and their relevance to tropical cyclone dynamics. In *Proc. ICSU/WMO Internat. Symp. on Tropical Cyclone Disasters Beijing* (ed. J. Lighthill, Z. Zheng, G. Holland & K. Emanuel), pp. 143–156. Beijing, Peking University Press.
- MCINTYRE, M. E. & NORTON, W. A. 1990 Dissipative wave-mean interactions and the transport of vorticity or potential vorticity. *J. Fluid Mech.* **212**, 403–435 (and Corrigendum **220**, 693).
- NORTON, W. A. 1988 Balance and potential vorticity inversion in atmospheric dynamics. PhD thesis, University of Cambridge, 167 pp.
- SHEPHERD, T. G. 1990 Symmetries, conservation laws, and Hamiltonian structure in geophysical fluid dynamics. *Adv. Geophys.* **32**, 287–338.
- WHITHAM, G. B. 1974 *Linear and Nonlinear Waves*. Wiley-Interscience, 620 pp.
- YIH, C. S. 1997 The role of drift mass in the kinetic energy and momentum of periodic water waves and sound waves. *J. Fluid Mech.* **331**, 429–438.